ACIBADEM MEHMET ALİ AYDINLAR UNIVERSITY
INSTITUTE OF HEALTH SCIENCES

INVESTIGATION OF THE FUNCTION OF VINCULIN AND ITS ISOFORM IN MUSCLE CELLS

HANDE KASAP CAN

M.Sc. THESIS

DEPARTMENT OF MEDICAL BIOTECHNOLOGY

SUPERVISOR
Assoc. Prof. Zeynep Aslıhan Durer

ISTANBUL-2022

ACIBADEM MEHMET ALİ AYDINLAR UNIVERSITY
INSTITUTE OF HEALTH SCIENCES

INVESTIGATION OF THE FUNCTION OF VINCULIN AND ITS ISOFORM IN MUSCLE CELLS

HANDE KASAP CAN

M.Sc. THESIS

DEPARTMENT OF MEDICAL BIOTECHNOLOGY

SUPERVISOR
Assoc. Prof. Zeynep Aslıhan Durer

ISTANBUL-2022

DECLARATION

I declare that this thesis work is my own work, I had no unethical behavior at any stages from the planning to the writing of the thesis, I obtained all the information in this thesis in accordance with academic and ethical rules, I cited all the information and comments that were not obtained with this thesis work, and I provided resources in the list of references. I also declare that there was no violation of any patents and copyrights during the study and writing of this thesis.

04/01/2022
Hande Kasap Can
İmza

PREFACE AND ACKNOWLEDGEMENT

First and foremost, I would like to thank my supervisor, Assoc. Prof. Zeynep Aslıhan Durer, for her time, patience, guidance and for giving me the opportunity to learn many things in her lab. I am also immensely grateful to Assoc. Prof. Devrim Öz Arslan for her suggestions and helps throughout this project.

My gratitude also goes out to all my colleagues; Demet Açıkgöz, Simge Şenay, Tuğçe Demir and Hande İpek Yetke; who supported and helped me through this journey.

I would like to thank warmly to my parents and my husband for their endless support and wise counsels.

I would also like to thank to Acibadem Mehmet Ali Aydinlar University for providing laboratory facilities and to Scientific and Technological Research Council of Turkey (TUBITAK) for their financial support.

This study was supported by TUBITAK 3501 project (118Z149); I was supported as a fellow from 2019 to 2020.

TABLE OF CONTENTS

LIST OF ABBREVIATIONS

ACTN1	Actinin alpha 1
APS	Ammonium persulphate
Arp2/3	Actin related protein 2/3 complex
ARVC/D	Arrhythmogenic right ventricular cardiomyopathy/dysplasia
BSA	Bovine serum albumin
CAP/Ponsin	Sorbin and SH3 domain-containing protein 1
CSRP3	Cysteine and glycine-rich protein 3
CT	C-terminus
DCM	Dilated cardiomyopathy
DMSO	Dimethyl sulfoxide
DTT	1,4-Dithiothreitol
EDTA	Ethylenediaminetetraacetic acid
F-Actin	Fibrous actin
FBS	Fetal Bovine Serum
H1	Helix 1
H9C2:	Rat myocardium cell line
HCl	Hydrochloric acid
HCM	Hypertrophic cardiomyopathy
ICDs	Intercalated discs
Iso/iso	Isoproterenol
KCl	Potassium chloride
kDa	Kilodalton
KH_2PO_4	Potassium dihydrogen phosphate
MHC-α	Myosin heavy chain, α isoform
ml	Milliliter
MLP	Muscle limp protein
mM	Millimolar
MVcl	Metavinculin
MVt:	Metavinculin tail domain
µg	Microgram

µl	Microliter
$Na_2HPO_4.12H_2O$	Sodium phosphate dibasic dodecahydrate
Na_3VO_4	Sodium orthovanadate
NaCl	Sodium chloride
NaF	Sodium fluoride
NaOH	Sodium hydroxide
NT	N-terminus
P	Proline-rich region
PBS	Phosphate buffered saline
PDB	Protein data bank
Pe	Phenylephrine
PEI-MAX	Polyethylenimine hydrochloride
PFA	Paraformaldehyde
PI	Protease inhibitor
PIP2	Phosphatidylinositol 4,5-bisphosphate
PMSF	Phenylmethanesulfonyl
PVDF	Polyvinylidene difluoride
RAVER1	Ribonucleoprotein, tract-binding protein 1
RCSB	Research Collaboratory for Structural Bioinformatics
RIPA:	Radioimmunoprecipitation assay
SDS	Sodium dodecyl sulfate
TCAP	Telethonin
TEMED	Tetramethyl ethylenediamine
TTN	Titin
VASP	Vasodilator stimulated phosphoprotein
VCL/Vcl	Vinculin
Vh	Vinculin head domain
Vt	Vinculin tail domain

LIST OF FIGURES

LIST OF TABLES

ÖZET

Kas Hücrelerinde Vinkülin ve İzoformunun İncelenmesi

Dünya Sağlık Örgütü'ne göre dünyada en çok kardiyak hastalıklardan ölüm gerçekleşmektedir. Türkiye İstatistik Kurumu (TUIK) da ölüm verileri içinde kalp hastalıklarının yüzdesinin gittikçe arttığını belirtmiştir. Kalp hastalıkları 1989'da %40, 1993'te %45, 2009'da %40, 2013'te %39,6 ve 2014 yılında %40,4 ile tüm ölüm nedenleri arasında birincidir. Kardiyomiyopati, kalp hastalıklarının önemli bir bölümünü oluşturan bir kalp kası hastalığıdır. Hem dilate hem de hipertrofik kardiyomiyopatilerle ilişkili genlerden biri, vinkülin proteinini kodlayan VCL'dir. Vinkülin, aktin hücre iskeletinin adezyon reseptörlerine bağlanmasında rol oynayan bir adaptör proteindir. Vinkülin, hücre dışı matristen sitoplazmaya kuvvet iletiminde işlev gören fokal adezyonlarda zenginleşmiş ve yaygın olarak bulunan bir proteindir. Vinkülinin kasa özgü bir izoformu olan metavinkülin, kostamerler, interkalasyonlu diskler ve yoğun plaklar dahil olmak üzere hücre yapışma noktalarında vinkülin ile birlikte bulunur. Metavinkülinin kas hücrelerinde hangi işlevi yerine getirdiği bilinmemesine rağmen, metavinkülin spesifik bölgesindeki nokta mutasyonları kalp hastalıkları ile ilişkilendirilmiştir. Bu çalışmanın amacı, bir kalp kası hücre hattında metavinkülinin aktin hücre iskeletini, fokal adezyonları ve hipertrofi yanıtını nasıl etkilediğini araştırılmasıdır. Bu kapsamda fare embriyonik kalp hücresi olan H9C2 hücre hattında metavinkülin ve vinkülin transfeksiyonu gerçekleştirilmiş ve transfekte hücre morfolojisindeki değişiklikler konfokal mikroskopi ve fokal adezyon analizi ile incelenmiştir. Protein seviyesindeki değişiklikleri tespit etmek için Western blot deneyleri yapılmıştır. Sonuç olarak, H9C2 hücrelerine hipertrofi ve fokal adezyon analiz yöntemleri başarıyla uygulandı ve vinkülin ve metavinkülinin hücre iskeleti organizasyonu üzerindeki etkileri gözlemlendi.

Anahtar Sözcükler: Vinkülin, Metavinkülin, Hipertrofi, Fokal adezyon, Kardiyomiyopati

ABSTRACT

Investigation of the Function of Vinculin and its Isoform in Muscle Cells

According to the World Health Organization, most deaths occur from cardiac diseases in the world. The Turkish Statistical Institute (TUIK) also stated that the percentage of heart diseases in mortality data is increasing gradually. Heart diseases are the first among all causes of death with 40% in 1989, 45% in 1993, 40% in 2009, 39.6% in 2013 and 40.4% in 2014. Cardiomyopathy is a disease of the heart muscle that accounts for a significant portion of heart diseases. One of the genes associated both with dilated and hypertrophic cardiomyopathies is VCL that encode for vinculin protein. Vinculin is an adaptor protein involved in the linkage of actin cytoskeleton to adhesion receptors. Vinculin is a ubiquitous protein enriched in focal adhesions functioning in transmission of force from the extracellular matrix to the cytoplasm. Metavinculin, a muscle-specific isoform of vinculin, is also found with vinculin at cell adhesion points including costameres, intercalated discs, and dense plaques. Point mutations in the metavinculin specific region have been linked to heart disease, despite the fact that it is unknown what function metavinculin performs in muscle cells. The aim of this study was to investigate how metavinculin affects actin cytoskeleton, focal adhesions and hypertrophy response in a cardiac muscle cell line. In this context, metavinculin and vinculin transfection were performed in the H9C2 cell line, which is a mouse embryonic heart cell, and the changes in transfected cell morphology were examined by confocal microscopy and focal adhesion analysis. Western blot experiments were performed to detect changes in protein level. In conclusion, hypertrophy and focal adhesion analysis methods were successfully applied to H9C2 cells and the effects of vinculin and metavinculin on cytoskeletal organization were observed.

Keywords: Vinculin, Metavinculin, Hypertrophy, Focal adhesion, Cardiomyopathy

1 INTRODUCTION

According to the World Health Organization, the number one cause of death in the world is cardiovascular diseases with 85% of these cardiovascular related deaths resulting from heart attack and stroke in 2016 (1) and almost one person dies every 36 seconds from the cardiovascular disorders in the United States (2).

Cardiomyopathy is a disease of the heart muscle cells called the myocardium. There are many types of cardiomyopathies including the familia types with genetic origin (3). Environmental, dietary, and genetic factors all play a role in the development of cardiovascular and cardiomyopathy diseases. Genetic mutations in the structural proteins that make up the intercellular and cell-extracellular matrix junctions in the heart cause abnormalities in cell functions or organ failure like cardiomyopathy.

There are primary and secondary classes of cardiomyopathy. Those of genetic origin fall into the primary group. The most common cardiomyopathies that causes death in the world are hypertrophic and dilated cardiomyopathy (3,4). A crucial information from identifying multiple pathogenic variations in genes of patients with hypertrophic and dilated cardiomyopathy is that the variations are often found in genes that encode the sarcomere protein constituents (3). Familial hypertrophic cardiomyopathy is associated with mutations found in distinct sarcomeric contractile proteins (4). On the other hand, mutations associated with dilated cardiomyopathy are found in sarcomeric and cytoskeletal proteins (5).

One of the genes known to be involved in these two most common types of cardiomyopathies is VCL. Vinculin is a cytoskeletal protein ubiquitously expressed that links transmembrane adhesion receptors to actin filaments and plays a central role in the management of cell adhesion, motility, and transmission of force (6).

Previous researches have shown that vinculin deficiency leads to the extreme weakening of the extracellular matrix and adhesion of cells, which eventually facilitates the proliferation of cancer and migration (7). Vinculin is involved in the

development of the cytoskeletal complex of actin that serves in both vascular inflammation and remodeling (8,9). It is crucial for focal adhesion formation and has active and inactive forms. Active form of vinculin is found at focal adhesions at membranes and it helps their regulations. For the protection of the epithelial barrier, which is accomplished by protecting endothelial junctions from opening during force-dependent remodeling, the sustaining of vinculin is critical (7). Vinculin is critical for the development and the function of the heart, including contraction, as well as cardiomyocyte adhesion functions. Vinculin knockout mouse embryos do not live after embryonic day 10 and have neural tube and heart developmental abnormalities. There are less adhesions on vinculin-null murine embryonic fibroblasts and therefore have defects in cell spreading and are less able to attach. So, they are more motile and avoid apoptosis and anoikis. In addition, dilated cardiomyopathies can be occurred by heterozygous vinculin deletion (+/-)(10).

Metavinculin, the long isoform of vinculin as a result of alternative splicing in muscle cells, is seen together with vinculin at cell adhesion points such as costameres, intercalated discs and dense plaques. Metavinculin is found exclusively in muscle cells of the smooth and cardiac muscles, and in platelets at low levels (11). By controlling cellular morphology, cellular motility, and the transducing force between adjacent cells as well as between cells and the extracellular matrix, vinculin and metavinculin play crucial roles in cell adhesion. Metavinculin expression throughout contraction is increased in muscle cells. In mice, dilated cardiomyopathy results from heterozygous inactivation or knockout of vinculin activation. Metavinculin point mutations are associated with both dilated cardiomyopathy and hypertrophic cardiomyopathy patients (12,13).

Family linkage tests have still not been reported, however, and the number of patients diagnosed with metavinculin mutations remains too limited to be clear evidence of cardiomyopathy-causing metavinculin dysfunction. The lack of metavinculin has not impaired cardiac development and function. The vinculin isoforms, however, display specific mechanical features (14,15).

The goal of this research is to learn more about how metavinculin influences the actin cytoskeleton, focal adhesions, and the response of H9C2 cells to hypertrophy. Metavinculin and vinculin transfection were carried out in the H9C2 cell line, which is a mouse embryonic heart cell, and confocal microscopy and focal adhesion analyses were performed to understand the changes in the cell shape and focal adhesions. To detect changes in protein levels, Western blot studies were carried out. Induction of hypertrophy in these cells allowed the observation of how the transient expression of metavinculin and vinculin affect cell shape and focal adhesions. As a result, we successfully applied previously established tools for focal adhesion analysis to H9C2 cells and made initial observations on how vinculin and metavinculin may alter these structures. As a future aspect, the use of stable cell lines instead of transient expression will provide a better understanding of the function of metavinculin on focal adhesion function.

2 BACKGROUND

2.1 Cardiomyopathy

Cardiomyopathies, which are not ischemic, that is, without any interruption of oxygen flow to any tissue or organ in the body, are a diverse group of cardiac diseases that often result in cardiac failure and death (3). Cardiomyopathy affects the heart muscle that cause pump abnormalities in the heart (16). This is a physiological and pathological condition related to heart muscle or electrical dysfunction. There are different causes of cardiomyopathy which are mainly inherited (5).

2.2 Classification

Cardiomyopathies are classified into two groups which are primary cardiomyopathies and secondary cardiomyopathies. Primary cardiomyopathies can be genetic, nongenetic or acquired. They are mostly related with heart muscle and they are few in number (17). Genetic cardiomyopathies resulting from an abnormality in the genes that impact the heart. Acquired cardiomyopathies involve nongenetic reasons that create cardiac problem. If genetic and nongenetic reasons combine these are mixed type of cardiomyopathies (18).

Secondary cardiomyopathies include myocardial involvement of multiorgan disorders (17).

Because of the many of the cardiomyopathy types related to heart but it is not limited to just heart, differences between primary and secondary cardiomyopathies are comparative and depend on the cruciality and its results of the myocardial process. Consequently, under the light of points mentioned above, the American Heart Association panel defined the cardiomyopathies as primary (genetic, mixed, acquired) and secondary (18).

Table 1. Classification of Primary Cardiomyopathies

Acquired
Myocarditis
Peripartum
Tachycardia induced
Takotsubo (stress induced)
Genetic
Arrhythmogenic right ventricular dysplasia
Hypertrophic
Ion channel disorders
Left ventricular compaction
Mitochondrial myopathies
Mixed
Dilated
Restrictive

Figure 1. Classification of primary cardiomyopathies (18).
(Primary cardiomyopathies can be acquired, genetic or mixed.)

The conditions are separated into genetic or nongenetic etiologies. Mixed cardiomyopathies are mostly nongenetic; familial history of disease is rare (18).

2.2.1 Primary cardiomyopathies (genetic)

2.2.1.1 Hypertrophic cardiomyopathy

Hypertrophic cardiomyopathy (HCM) is a heterogeneous type of cardiac disease that is genetically autosomal dominant and involves mutation of genes that encodes sarcomeric proteins (3,12,18). 1:500 patient that has disease phenotype is HCM. This shows that the HCM is the most common cardiomyopathy type. Data from the United States of America demonstrates that HCM is the most common cause of sudden cardiac death in the young, even in athletes, and it is a very important factor for heart failure disability at every age of people (3,12).

HCM morphologically seen as a hypertrophic heart without any of the secondary diseases and chamber dilation that cause heart thickening and nondilated left ventricle (3,18).

It has some pathological markers like myocyte growth and disarray, and the increased myocardial fibrosis. Sometimes disarray of myocytes can be seen in other types of cardiomyopathies but the ratio for HCM is much higher (19).

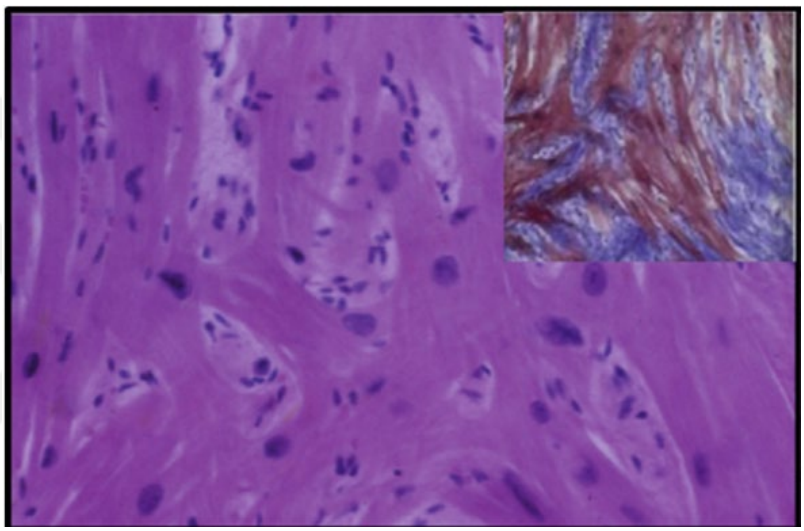

Figure 2. Normal and pathologic myocardial histology HCM (19).

Hypertrophic cardiomyopathy is characterized by obvious myocyte disarray, interstitial fibrosis and hypertrophy. It increased interstitial fibrosis can be seen with blue which is the Masson trichrome stain. This stain is used in histological staining which is distinguishing cells from surrounding connective tissue (19).

2.2.1.2 Arrhythmogenic right ventricular cardiomyopathy/dysplasia

Arrhythmogenic Right Ventricular Cardiomyopathy/Dysplasia (ARVC/D) is an uncommon type of genetic heart disease that seen approximately 1:5000 ratio (3). Additionally, half of the patients got sick with genetic factors (18). ARVC/D patients usually suffer from myocytes loss especially in the right ventricle of the heart and fatty or fibrofatty which means fibrous and fatty tissue replacement. This causes regional or

total abnormalities in the heart. Typically, it is related with myocarditis which is heart muscle inflammation because of adenovirus or enterovirus in some cases. Still, it is not included in inflammatory primary cardiomyopathies (3).

One of the characteristic symptoms of ARVC/D is ventricular tachyarrhythmias which is disturbance of the heart's rhythm characterized by rapid and irregular beating. It is a sudden cardiac death reason for young, also for example it is the most common cause of sudden death for athletes in Italy (3).

Most of the times, ARVC/D is autosomal dominant although often with incomplete penetrance (3).

2.2.2 Mixed cardiomyopathies (genetic and nongenetic)

2.2.2.1 Dilated cardiomyopathy

Dilated cardiomyopathy (DCM) is the situation of ventricular chamber enlargement and systolic dysfunction with normal left ventricle wall thickness (3).

Dilated cardiomyopathy causes progressive heart failure, arrhythmias in ventricles and above the ventricles of the heart, conduction system failures, thromboembolism which means a clot fragment from a thrombus in a vein causing a blockage in another region of the vein, and sudden or heart failure related death. It is a common irreversible disease that has prevalence of 1:2500. Also, it is the third most common cause of heart failure and the most frequent cause of heart transplantation. DCM can be seen at any age and it has very severe and limiting symptoms (3).

DCM can be occurred primary (genetic) or secondary (nongenetic) factors like infectious agents particularly viruses that often-producing myocarditis, bacterial, fungal, mycobacterial and parasitic. Other reasons are toxins, excessive alcohol usage, autoimmune and systemic disorders, some chemo therapeutic agents, metals and other compounds like cobalt, lead, mercury, and arsenic, neuromuscular disorders and

mitochondrial, metabolic, endocrine, and nutritional disorders like selenium deficiencies (3).

About 20% to 35% of the DCM patients are genetic although with incomplete or age-related penetrance. It is genetically heterogeneous but still autosomal dominant, with X-linked autosomal recessive and mitochondrial inheritance less frequent (3).

Some of the dominant mutant genes that related to DCM encode the same contractile sarcomeric proteins that related with HCM like α-cardiac actin (3).

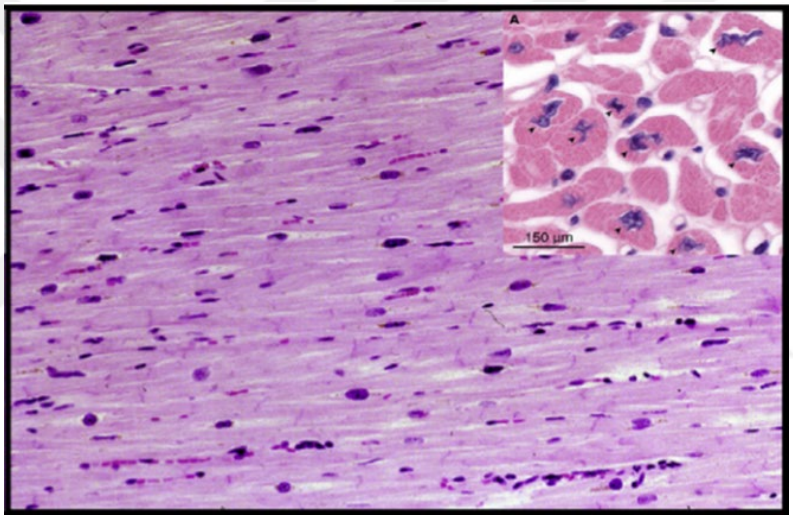

Figure 3. Normal and pathologic myocardial histology DCM (19).

(Non-specific anomalies like slightly elevated interstitial fibrosis but not myocyte and myofibrillar disarray describe dilated cardiomyopathy. Often found are myocyte nuclei with an irregular morphological characteristic (arrowheads))

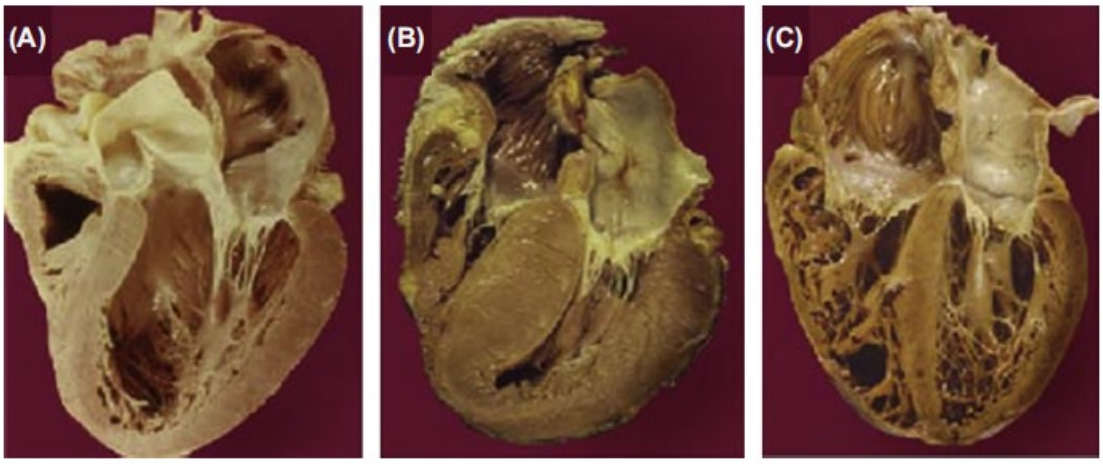

Figure 4. Normal and pathologic myocardial gross anatomy (19).

(This image shows the differences between normal, HCM and DCM heart anatomy. A show the myocardium that has a normal left ventricle wall thickness (≤11 mm) and normal left ventricle volume. In B, increased left ventricle wall thickness without cavity dilation. And C demonstrates the dilated cardiomyopathic heart with the growth of the left ventricle)

2.2.2.2 Restrictive cardiomyopathy

It is a rare type of cardiomyopathies that 2% to 5% of the patients have this disease. It is resulting from increased myocardial stiffness. It can be primary or secondary with amyloidosis, sarcoidosis, radiation therapy etc. (18).

2.2.3 Secondary cardiomyopathies

If there is a secondary cause of heart disease in the patient, this disease is called secondary cardiomyopathy. Secondary causes might be excessive alcohol usage, autoimmune disorders, endocrine, toxic, and infectious (18).

Table 2. Secondary Causes of Cardiomyopathy

Autoimmune/inflammatory	**Infiltrative disorders**
Dermatomyositis	Amyloidosis
Polyarteritis nodosa	Gaucher disease
Rheumatoid arthritis	Hunter syndrome
Sarcoidosis	Hurler syndrome
Scleroderma	**Neuromuscular and storage disorders**
Systemic lupus erythematosus	Glycogen storage disorders
Endocrine	Muscular dystrophy (Becker, Duchenne, Emery-Dreifuss, myotonic)
Acromegaly	Neurofibromatosis
Diabetes mellitus	**Nutritional deficiencies**
Hyperparathyroidism	Kwashiorkor
Hyperthyroidism	L-carnitine, niacin, selenium, thiamine, vitamin C deficiencies
Hypothyroidism	**Toxic**
Obesity	Alcohol
Infectious	Anabolic steroids
Chagas disease	Chemotherapeutic agents (anthracyclines, cyclophosphamide, doxorubicin [Adriamycin])
Hepatitis C	Chloroquine (Aralen)
Human immunodeficiency virus	Heavy metals (arsenic, cobalt, lead, mercury)
Mycobacteria	Iron excess (hemochromatosis)
Rickettsia	Radiation
Viral (adenovirus, Coxsackie, Epstein-Barr, parvovirus)	Stimulants (cocaine, methylphenidate)

Figure 5. Secondary causes of cardiomyopathy (18).

(It is referred to as secondary cardiomyopathy if the patient has a secondary source of heart disease like denoted in figure 5. (18)

2.3 Genetics of Cardiomyopathy

A critical disclosure from the distinguishing proof of numerous pathogenic variations in cardiomyopathy genes from various cardiomyopathy patients is that illness genes frequently encode the protein constituents of the sarcomere. Pathogenic variant which are related with sarcomere proteins are the most common reasons of hypertrophic and dilated cardiomyopathy (19).

Sarcomere is the basic unit that allows all muscle cells to contract. Sarcomere proteins are organized into thick (myosin heavy and light chains) and thin (actin, troponin complex and α-tropomyosin) filaments intertwined during muscle fiber shortening and elongation. Interaction between actin and myosin is the basis of contraction and relaxation (19).

2.3.1 Genetics of HCM

HCM generally follows an autosomal dominant inheritance pattern characterized by significant differences in expression and age-related penetration (4).

HCM actually happens through the eight major sarcomeric mutations that encode different parts of contractile apparatus (19). It happens because of missense mutations in cardiac sarcomere but sometimes nonsense, frameshift, and in-frame insertion/deletion mutations can also be seen (4).

Unlike DCM, which is primarily an adult-onset disease, HCM, caused by mutations in genes encoding sarcomeric proteins, most commonly occurs during adolescence (4).

HCM is inherited as an autosomal dominant trait conveying a risk of transmission to descendants of 50%. Linkage testing of large HCM genera identified disease loci on chromosomes 1, 11, 14, and 15 where various proteins of the contractile apparatus are encoded (19,20).

The definition of HCM is generally limited to hypertrophy caused by mutations in genes encoding sarcomeric contraction proteins. Other non-syndromic, genetic causes of the hypertrophic phenotype are additionally addressed by this nomenclature (4).

Family research and subsequent genetic epidemiological analyzes have shown that in approximately 60 percent of patients with clinical requirements for HCM, pathogenic or likely pathogenic variants in sarcomere protein genes exist. Recently, sequence analyzes of about 18 genes involved in unexplained hypertrophy reported the increased prevalence of sarcomere-altering variants in patients relative to a large population reference dataset of 60,706 subjects (19).

The clinical significance of certain genes that are found to be connected with HCM has not yet been fully determined due to a lack of strong evidence that they are

definitive. These include α-actinin (ACTN1), α-MHC (MYH6), MLP (CSRP3), telethonin (TCAP), titin (TTN), and vinculin (VCL).

Table 1 Molecular Substrate of HCM

Strongest evidence for pathogenicity	
Thick filament	
1. β-myosin heavy chain	MYH7
2. Regulatory myosin light chain	MYL2
3. Essential myosin light chain	MYL3
Thin filament	
4. Cardiac troponin T	TNNT2
5. Cardiac troponin I	TNNI3
6. Cardiac troponin C	TNNC1
7. α-tropomyosin	TPM1
8. α-cardiac actin	ACTC
Intermediate filament	
9. Cardiac myosin-binding protein C	MYBPC3
Z-disc	
10. α-actinin 2	ACTN2
11. Myozenin 2	MYOZ2
Lesser evidence for pathogenicity	
Thick filament	
12. α-myosin heavy chain	MYH6
13. Titin	TTN
Z-disc	
14. Muscle LIM protein	CSRP3
15. Telethonin	TCAP
16. Vinculin/metavinculin	VCL
Calcium handling	
17. Calsequestrin	CASQ2
18. Junctophilin 2	JPH2

HCM = hypertrophic cardiomyopathy.

Figure 6. Molecular substrate of HCM (20).
(Strongest and lesser evidences for pathogenicity of HCM genes are demonstrated)

2.3.2 Genetics of DCM

Synchronized and compatible heart contractions are promoted by matching of sarcomeres at Z bands, adjacent myocytes at intercalated discs, and myocytes and the extracellular matrix at costameres and dystrophin glycoprotein complexes. In these areas, mutations in proteins that help the transmission of contractile forces may alter contractions resulting in mechanical cellular damage, and progressive heart failure (21).

Starting of familial dilated cardiomyopathy generally is 30s to 50s but it can even be seen babies, children and elders. Familial studies have shown that familial dilated cardiomyopathy can quietly be found in a patient for years without symptoms (4).

Mutations in genes that cause DCM mostly divided into two types of protein which are cytoskeletal and sarcomeric proteins. Dystrophin, desmin, lamin A/C, ɑ-sarcoglycan, ß-sarcoglycan, and vinculin/metavinculin are among the cytoskeletal protein group (5). Metavinculin deficiency or decrease in its expression levels are linked to dilated cardiomyopathy or plaque arrangement, respectively, during human coronary arteriosclerosis (15).

More than 20 genes representing significant locus heterogeneity have been identified as causes of DCM. Most of these genes are allelic heterogeneous. The genes involved in DCM code for a variety of proteins expressed in the cardiomyocyte, ranging from nuclear envelope, cardiac sarcomere, ion channels, transcription factors, and dystrophin-associated cytoskeletal complex (4). Also, mitochondrial defects are also possible.

The impact of the familial dilated cardiomyopathy is highly variable and depends on the age. Impact predictions are 10% at 20 years, 34% between 20 to 30 years, 60% between 30 to 40 years, and 90% at 40 years (4).

	Gene	Protein	Protein location
Xp21.2	DMD	Dystrophin	Cytoskeleton/SL
Xq28	G4.5	Tafazzin	Phospholipid
1q12	TNNI1	Cardiac troponin I	Sarcomere
1q32	TNNT2	Cardiac troponin type 2	Sarcomere
2q31	TTN	Titin	Sarcomere
2q35	DES	Desmin	Cytoskeleton
5q34	SGCD	δ-sarcoglycan	Cytoskeleton/SL
6q12–q16	CMD1K	Unknown	Unknown
6q22.1	PLN	Phospholamban	Calcium
9q13-q22	CMD1B	Unknown	Unknown
9q22-q31	SEMA4D	Unknown	Unknown
10q22.1	MYPN	Myopalladin	Sarcomere
10q22.3–23.2	ZASP/Cypher (LDB3)	LIM domain binding protein 3	Sarcomere
1q42–q43	α2-actinin	ACTN	Sarcomere
10q22.1–q23	VCL	Metavinculin	Cytoskeleton
10q23.22	ANKRD1	CARP	Sarcomere
10q25.3	RBM20	RNA binding motif protein 20	Unknown
11p11.2	MYBPC3	Myosin binding protein C	Sarcomere
11p15.1	CSRP3	Muscle-LIM protein	Sarcomere
14q11.2–q13	MYH7	β-myosin heavy chain	Sarcomere
15q11–q14	ACTC1	Cardiac actin	Sarcomere
15q22.1	TPM1	α-tropomyosin	Sarcomere

Table: Genetic causes of dilated cardiomyopathy by chromosome locus

Figure 7. Genetic causes of DCM by chromosome locus (5).

(Gene, protein and protein location to trigger DCM is demonstrated)

Mutations in the sarcomere can cause DCM or HCM. Sarcomeric gene mutations that cause DCM are also cause HCM like ß-myosin heavy chain, myosin-binding protein C, actin, α-tropomyosin, cardiac troponin T and C. Sarcomeric genes, those encoding Z-disk proteins, also identified ZASP, muscle-LIM (lin11, isl-1, and mec-3) protein, α-actinin-2, myopallidin, cardiac ankyrin repeat protein, and telethonin, phospholamban, tafazzin, and the sodium-channel gene SCN5A44 (5).

2.4 Vinculin and Metavinculin

2.4.1 Vinculin

Vinculin is a cytoskeletal protein that is found in adherent junctions and focal adhesions and is required for their function (15,22). It is found in chromosome 10 q22.1-q23 and includes 22 exons. Exon 19 is alternately spliced with tissue specific expression. The smaller isoform, vinculin, is ubiquitously expressed (12,21). Most of the vinculin ligands are adhesion proteins or cytoskeletal proteins (15). It links adhesion receptors to actin filaments like a scaffold and it is participates in processes such as motility, cell adhesion, and force transmission between cells and cell-matrix interface (22). In addition to its role in cell-matrix bonds, vinculin is also present in cell-cell adhesion junctions connecting one cell to another (23). Without vinculin, defects in heart and nerve formation occur, and mouse embryos fail to survive after day 10. Also, absence of vinculin cause resistance to apoptosis and anoikis which is an apoptosis induced by lack of correct cell/extracellular matrix attachment, rounded morphology, increased motility (24).

Vinculin is a molecular scaffold protein with a molecular weight of 117 kDa (15,23,25). It has a head domain that is 90 kDa, a flexible proline-rich linker and a tail domain at the molecular level. As part of its scaffolding role, Vcl interacts with a variety of cytoskeletal and adhesion proteins, as well as 4, 5-bisphosphate phosphatidylinositol (PIP2). Vcl head domain interplays with the α-catenin at cell-cell junctions, talin at focal adhesions and α-actinin at both cellular locations. The proline-rich linker attaches Vcl head domain to tail domain. Also, it may interact with a variety

of cytoskeletal proteins for example, VASP, CAP/ponsin, Arp2/3 complex and vinexin. Vcl tail directly attaches to F-actin, PIP2, paxillin and Raver1 (22).

Internal flexibility assists to association and dissociation of vinculin with itself, and other proteins in the cytoplasm and cell membrane. Vinculin head and tail domains' intramolecular interactions allows the regulation of the accessibility of binding sites with other protein partners. In the active state, vinculin is weakly folded, allowing it to bind to other proteins at cell adhesion sites (12). Vinculin interactions attach the actin cytoskeleton to membrane adhesion structures (17).

2.4.2 Metavinculin

Metavinculin (MVcl) is a larger Vcl splice isoform exclusively expressed in smooth, cardiac and skeletal muscle cells, and low levels in platelets (12,15,21,23,25). For proper functioning, cardiac and smooth muscle cell forms display a high degree of contractility, with increased metavinculin production contributing to the contractile load on the tissue (13). Metavinculin localizes with vinculin at dense plaques in smooth muscles, intercalated discs in cardiomyocytes and costameres in skeletal muscles. Half of the vinculin can be found as metavinculin in smooth muscles (26). Because metavinculin expression is increased with muscle differentiation and it is specific for muscle types, this demonstrates the metavinculin is attendant for the contractility (27). MVcl is expressed at sub-stoichiometric rates (9–42%) comparative to Vcl (22,23). If only vinculin is present without metavinculin, a wide network of thick F-actin fibers would cause the heart muscle to become rigid and would not maintain the requisite contractile properties. Therefore, metavinculin co-expression may reduce the bundling of vinculin-mediated actin so that the cardiac cells remain stable and functional, functioning as a molecular rheostat. Reduced levels of metavinculin expression are correlated with cardiomyopathy and disorganized intercalated disk structures, indicating the need for metavinculin to maintain smooth muscle actin-membrane adhesion sites and to produce and transmit force via its interaction with the actin cytoskeleton (25). The expression correlates to the high contractile needs of certain muscle cells (22). Studies have shown that metavinculin forms a different F-actin

supra-organization than vinculin, with fine-textured F-actin filaments organized by metavinculin compared to larger vinculin bundles. These results show that the ratio of metavinculin to vinculin in intercalated discs or other cellular structures likely affects the stiffness of cells through actin organization (23). It has also been proven that altered expression or mutation of metavinculin can lead to cardiac dysfunction and attribute metavinculin abnormalities to both dilated and hypertrophic forms of human cardiomyopathy (23). Metavinculin and its functions are still not fully understood (15).

2.4.3 Importance and role of vinculin and metavinculin in terms of cardiomyopathy

Since they are contractile cells, cardiac myocytes are basically under constant mechanical stress. Cell-cell and cell-matrix junctions in cardiac myocytes are termed intercalated discs (ICDs) and costameres, respectively. Vinculin and metavinculin is part of these structures (23).

It is found that the vinculin expression in failing heart is increased in humans. This shows that the vinculin expression can be increased to support insufficient heart cells (23).

One of the serious health issues is the debilitation of cardiac problems arising from cardiomyopathies. As many as 1 in 500 adults could have this disorder according to the Centers for Disease Control and Prevention. It has been shown that both DCM and HCM are correlated with genetic and sporadic mutations in genes which code the cardiac tissue-specific vinculin isoform, metavinculin (25).

Total knockout or heterozygous inactivation of the Vcl gene is correlated with dilated cardiomyopathy in mice whereas decreased expression of MVcl is also correlated with dilated cardiomyopathy (DCM) and disorganized intercalated disc structures in humans. Additionally, MVcl point mutations are observed with the patients have DCM and HCM. A934V and ΔL954 mutations in MVcl are related with DCM. R975W mutation is related with the both DCM and HCM.

2.4.4 Structures of vinculin and metavinculin

Vcl and MVcl have same head domain but different tail domains. Vinculin tail domain (Vt) has an N-terminal strap, a 5-helix bundle and a C-terminal hairpin. On the other hand, MVcl tail domain includes an additional exon that encodes a 68 amino acid insert. MVcl tail has a 5-helix bundle fold like Vcl tail. The sequence that makes the helix 1 (H1) and the strap of Vcl tail is replaced in the MVcl tail with homologous sequences that is seen with an extra H1' domain insert (22).

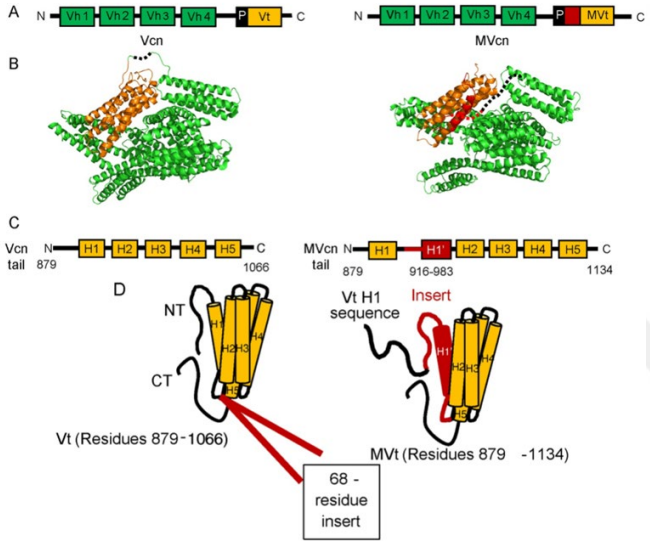

Figure 8. Sequence and structural differences between Vcl and MVcl (22).

(A demonstrates comparison of domain architecture for full-length Vcl and MVcl. B shows the crystal structures of Vcl and MVcl PDB data that are obtained from RCSB protein data bank. In the C diagram compares the sequence differences in the Vcl and MVcl tail domains. MVcl tail contains an insert of 68 amino acids between residue 915 and 916 (H1' in red, residues 916–983). D is the structural schematic figures sequence differences that lead to a helix replacement of H1 with H1' (red) in MVcl tail (Vh: Vcl head domain; Vt: Vcl tail domain; MVt: MVcl tail domain H: helix; NT: N-terminus; CT: C-terminus; and P: proline-rich region))

Similar to the Vcl tail domain, MVcl tail binds F-actin directly, however unlike Vcl tail domain, MVcl tail does not in vitro bundle filamentous actin into higher order structures. Nevertheless, because MVcl and Vcl are co-expressed in muscle tissues together, actin filament organization is likely to be regulated coordinately. The existence of MVcl tail at sub-stoichiometric levels impairs Vcl tail mediated F-actin

bundling; indicating that Vcl tail mediated actin bundling may be adversely controlled by MVcl tail (22).

MVcl loses expression in cell culture in smooth and cardiac muscle cells, without careful mimicking of the contractile environment (28). Lee et al. demonstrates that MVcl expression correlates to a greater effect individual focal adhesion region, faster cell migration, and reduced cell stiffness in response to external force compared with Vcl-expressing cells. They have shown that actin bundling mediated by Vcl in vitro is diminished as the concentration of MVcl tail increases. These results indicate that MVcl can play a big role in limiting transmission of force through Vcl tail-mediated actin bundling, rather than strengthening it. MVcl tail has similar binding actin filament characteristics as Vcl tail, but it does not dimerize and thus does not bundle actin filaments (22).

They also have shown that whereas Vcl tail can organize actin filaments into parallel bundles, on the other hand, MVcl tail arranges actin filaments instead of bundles into a mesh-like network. The existence of the insert, including H1', restricts MVcl tail's ability to bundle F-actin, since deleting H1' promotes actin filament bundling. The discrepancy between the two proteins in actin filament cross-linking possibly plays a role in how cells control focal adhesion and force transmission (22).

Head part of both vinculin and metavinculin interact with membrane associated ligand proteins and their tail part includes actin filament binding sites. Past in vitro studies illustrated differential geometric organization of actin fibers by the tail space of each isoform, recommending metavinculin may have a crucial part in securing actin fibers to intercalated circles within the heart. Also, in vitro assays show that when the mechanical loading occurs, vinculin expression is upregulated and vinculin disruption causes the contractile loss in the heart of mice embryos (23). Point mutations of metavinculin that are linked to dilated cardiomyopathies causes altered actin organization and ultrastructures of patient tissues showed disrupted intercalated discs (21).

Durer et al. shows that Mvt changes mechanical features of F-actin and increase the tendency of breaking of pieces of filaments with MVt. Because of the Mvt is a muscle specific protein, changes in actin filaments can be a mechanism for sense the load. Metavinculin serves as a controller of actin filament mechanics and of the structure encouraged by Vcl (25).

The expression of metavinculin in varying amounts, especially in muscle cells and depending on the developmental stages or muscle fiber type, indicates that metavinculin contributes to the contractile-sensitive rearrangement of F-actin in these cells. Furthermore, MVT binding changes the mechanical properties of actin filaments which can predispose the filaments to breakdown due to mechanical load. The latter is presumably critical for muscle development and maturation. Also, MVT adjusts the density and thickness of the actin filament bundles created by Vcl. MVT changes the VT-powered filament structure but does not alter the mechanical properties of filaments made with VT. Local density differences between metavinculin and vinculin can result in different mechanical properties of F-actin (15).

3 MATERIALS AND METHODS

3.1 Materials

Table 1. List of products and suppliers

Products	Suppliers
0% Fat Skim milk	Regilait
0,25% Trypsin-EDTA	Gibco
1,4-Dithiothreitol (DTT)	Applichem
2-mercaptoethanol	Sigma Aldrich
40% Acrylamide/Bis-acrylamide	Serva
Acetic acid (CH_3COOH)	Sigma Aldrich
Alexa Fluor® 488 Phalloidin	Cell Signaling Technology
Amersham Protran 0,2 µm NC membrane	GE Healthcare
Ammonium persulphate (APS)	Sigma Aldrich
Anti-rabbit IgG, HRP linked Antibody	Cell Signaling Technology
Bovine Serum Albumin (BSA) Fraction V	Roche
Bromophenol Blue	Sigma Aldrich
Calcium chloride (CaCl2)	Sigma Aldrich
CellMask™ Deep Red Plasma Membrane Stain	Thermo Fisher Scientific
Chambered coverslip µ-Slide 8 Well	Ibidi
Coomassie brilliant blue	Amresco
Dimethyl Sulfoxide (DMSO)	Sigma Aldrich
DMEM 1X 4,5 g/L D-Glucose, L-Glutamine, Pyruvate	Gibco
DNA Gel Loading Dye Purple (6x)	BioLabs
DpnI enzyme	BioLabs
Dulbecco's Phosphate Buffered Saline (dPBS)	Gibco
EDTA-free protease inhibitor cocktail (PI)	Roche
Ethanol	Sigma Aldrich
Ethylenediaminetetraacetic acid (EDTA)	Sigma Aldrich
Fetal Bovine Serum (FBS)	Gibco
GeneRuler 100 bp DNA Ladder	Thermo Fisher Scientific
Glycerol	Sigma Aldrich
Glycine	Serva
HEPES Buffer Solution	BI (Biological Industries)
Hydrochloric acid (HCl)	Sigma Aldrich
Igepal CA-630	Sigma Aldrich
Isoproterenol hydrochloride	Sigma Aldrich
Kanamycin	GeneMark
LB Broth	Serva
Lipofectamine 3000 reagent	Thermo Fisher Scientific
Magnesium chloride (MGCl2)	Sigma Aldrich
mEmerald-N1 plasmid	Addgene
mEmerald-Vinculin-N-18 plasmid	Addgene
Methanol	Sigma Aldrich

Table 1. List of products and suppliers (continued)

Products	Suppliers
Mouse monoclonal anti-β-Actin antibody	Sigma Aldrich
Opti-MEM Reduced Serum Media	Gibco
PageRuler™ Plus Prestained Protein Ladder, 10 to 250 kDa	Thermo Fisher Scientific
Paraformaldehyde	Sigma Aldrich
Penicillin-Streptomycin	Gibco
Peroxidase Affinipure Goat Anti-Mouse IgG (H+L)	Jackson ImmunoResearch
Phenylephrine hydrochloride	Sigma Aldrich
Phenylmethanesulfonyl fluoride (PMSF)	Applichem
Phosphoric acid (H3PO4)	Sigma Aldrich
Polyethylenimine Hydrochloride (PEI-MAX)	Polysciences
Potassium chloride (KCl)	Sigma Aldrich
Potassium dihydrogen phosphate (KH2PO4)	Sigma Aldrich
Primers (Forward and Reverse)	Sentebiolab
PVDF membrane 0,45 µm	Thermo Fisher Scientific
Pwo Master	Roche
Rabbit anti-FAK antibody	Cell Signaling Technology
Rabbit anti-vinculin antibody	Cell Signaling Technology
Rabbit monoclonal anti-α-Actinin antibody	Cell Signaling Technology
Rabbit monoclonal anti-Talin-1 antibody	Cell Signaling Technology
Rhodamine Phalloidin Reagent	Abcam
SDS	Sigma Aldrich
Sodium azide	Sigma Aldrich
Sodium chloride (NaCl)	Sigma Aldrich
Sodium fluoride (NaF)	Sigma Aldrich
Sodium hydroxide (NaOH)	Sigma Aldrich
Sodium orthovanadate (Na3VO4)	Sigma Aldrich
Sodium phosphate dibasic dodecahydrate	Sigma Aldrich
SuperSignal™ West Pico Plus Chemiluminescent Substrate	Thermo Fisher Scientific
TEMED	Sigma Aldrich
Triton X-100	NeoFroxx
Trizma Base	Sigma Aldrich
Trypan Blue Solution	Sigma Aldrich
Tween-20	Sigma Aldrich
Western blotting filter extra thick paper	Thermo Fisher Scientific
ZymoPURE™ Plasmid Miniprep Kit	Zymo Research
Zymo Mix&Go E. coli Transformation Kit	Zymo Research

Table 2. List of equipment

Equipment	Brand
-20°C freezer	Kirsch
-80°C freezer	GLF
4°C fridge	Kirsch
Biosafety cabinet	Thermo Fisher Scientific

Table 2. List of equipment (continued)

Equipment	Brand
Cell culture incubator	Esco
Centrifuge	Thermo Fisher Scientific
ChemiDoc MP Imaging System	Bio-Rad
Confocal microscope	Zeiss LSM 700
Environmental shaker/incubator	ESCO
Flow cytometer	BD FACSVerse
Fluorescence microscope	Zeiss
Inverted microscope	Zeiss
Micro centrifuge	Thermo Fisher Scientific
NanoDrop Spectrophotometer	Thermo Fisher Scientific
Nitrogen Tank	Thermo Fisher Scientific
Plate reader	BioTek
Thermal Cycler T100	Bio-Rad
Trans-blot turbo transfer system	Bio-Rad
Varioskan flash	Thermo Fisher Scientific
Water bath	Nüve

3.1.1 Preparation of chemicals, buffers and solutions

Protease Inhibitor (PI) (25x)

Roche complete EDTA-free protease inhibitor cocktail was dissolved in 2 ml of ddH_2O. 1 tablet of dissolved inhibitors is equivalent to 25x stock. The solution was aliquoted as 100 µl, aliquots were stored at -20°C. Before protein isolation, 25x PI was diluted with RIPA buffer to make 1x final.

Table 3. Polyacrylamide separating gels 12.5% (1x)

40% Acrylamide/Bisacrylamide	3,13 ml
1,5 M Tris (pH: 8.8)	2,5 ml
10% SDS	100 µl
ddH_2O	4,22 ml
10% APS	100 µl
TEMED	10 µl
Total volume	10 ml

Table 4. Polyacrylamide separating gels 8% (1x)

40% Acrylamide/Bisacrylamide	2 ml
1,5 M Tris (pH: 8.8)	2,5 ml
10% SDS	100 µl
ddH_2O	5,29 ml
10% APS	100 µl
TEMED	10 µl
Total volume	10 ml

Laemmli Loading Buffer (5x)

- 250 mM Tris-HCl (pH 6,8)
- 5% SDS
- 50% Glycerol
- 0,5% Bromophenol Blue
- Before using, 5% 2-Mercaptoethanol was added on the tube to avoid evaporation.

Bromophenol Blue (1%)

- 0,1 g bromophenol blue
- 10 ml methanol
- It was vortexed and filtered.

Bjerrum Schafer-Nielsen Transfer Buffer (10x)

- 48 mM Tris
- 39 mM Glycine
- 20% methanol
- 10x stock was diluted with ddH_2O to obtained 1x and 20% of total volume is methanol.

PBST (1x)

- 1x PBS
- 1% Tween-20

PBS (10x) (pH: 7.4)

- 1,37 M NaCl
- 0,03 M KCl
- 0,035 M KH_2PO_4
- 0,1 M $Na_2HPO_4.12H_2O$
- Completed with ddH_2O

Tris-HCl (1M pH:7.4)

- For 100 ml Tris-HCl preparation:
- 12,114 g Tris
- 50 ml ddH_2O
- HCl until the pH reached to 7,4
- Completed 100 ml with ddH_2O

RIPA Lysis Buffer (1x)

- 1 M Tris-HCl (pH:7,4)
- 5 M NaCl
- 0.5 M EDTA
- 200 mM NaF
- 100 mM Na_3VO_4
- 10% Igepal CA-630
- 10% Triton X-100
- 50 mM PMSF
- 1 M DTT
- dH_2O

4% Paraformaldehyde (pH: 7,2)

- Paraformaldehyde
- dPBS
- It was adjusted pH to 7,2.

Bradford Assay (1 L)

- 100 mg Coomassie Brilliant Blue
- 50 ml 95% Ethanol
- 100 ml 85% Phosphoric Acid
- Completed with ddH_2O

Running Buffer (10x)

- 0,25 M Tris Base
- 1,92 M Glycine
- After pH adjustment to 7,4 – 8,5, 1% SDS is added.
- Completed with ddH_2O

Staining Solution

- 50% Methanol
- 10% Acetic Acid
- 40% ddH_2O
- 1 gr Coomassie Brilliant Blue

Destaining Solution

- 40% Ethanol
- 10% Acetic acid
- 50% ddH_2O

BSA for primary antibodies 5%

- 5% (w/v) Fraction V BSA
- 1x PBS
- 0,02 % sodium azide

Isoproterenol (10 mM)

- For the 10 mM stock, 0,0025 gr iso was weighted and dissolved in 1 ml of dH_2O. Then, it was filtered and aliquoted as 15 µl. It was stored at -80°C.

Phenylephrine (20 mM)

- For the 20 mM stock, 0,004 g pe was weighted and dissolved in 1 ml of dH_2O. Then, it was filtered and aliquoted as 15 µl. It was stored at -80°C.

Alexa Fluor® 488 Phalloidin (6,6 µM)

- According to protocol, concentration should be 6,6 µM and 1:20 diluted in dPBS. Stock concentration was 100 µM. The dye was prepared according to these conditions and the number of wells to be stained for that experiment was calculated.

Rhodamine Phalloidin Reagent

- The main stock with a concentration of 1000X was used in 1% BSA with its concentration adjusted to 1X with PBS.

LB Broth (1 Liter)

- 25-gram LB broth was added to 1-liter ddH_2O then it was autoclaved.

Live Cell Imaging Solution

- 140 mM NaCl
- 2,5 mM KCl
- 1,8 mM $CaCl_2$
- 1 mM $MgCl_2$
- 20 mM HEPES
- It was adjusted pH to 7,4. Solution was used after filtration.

CellMask™ Deep Red Plasma Membrane Stain

- The main stock with a concentration of 1000X was used in live cell imaging solution with its concentration adjusted to 1X.
- 1X CellMask Plasma membrane stain was given to cells for 7 minutes at 37°C.

3.2 Methods

3.2.1 Cell culture

H9C2 (2-1) cardiomyocyte cells were obtained from ATCC (CRL-1446). The cells were cultured in 4,5g/L D-Glucose with pyruvate DMEM medium supplemented with 1% penicillin-streptomycin and 10% heat inactivated and sterile fetal bovine serum (FBS) in a humidified atmosphere of 5% CO_2 at 37ºC. The medium was changed every 2-3 days. The cells were passaged when they reached 70% confluency.

3.2.2 Transfection optimization

3.2.2.1 Choosing of transfection reagent and dose optimization

In H9C2 cells, in order to determine the optimal transfection agent: plasmid DNA ratio and time, cells were observed in fluorescence microscopy at 48-72 hours after transfection.

First, it was tested to determine the most appropriate agent and dose for H9C2 by trying different doses of transfection with Lipofectamine 3000 and Pei-MAX agents. For several weeks, different doses were tried by increasing or decreasing the transfection agent or plasmid doses in 96 well, 24 well and 6 well.

Transfection was performed by manufacturer's protocol. Briefly, with Lipofectamine 3000, Opti-MEM reduced serum media and lipofectamine 3000 agent were mixed in a test tube. In the other tube, the recommended dose of plasmid was diluted with p3000 reagent in the Opti-MEM media. The two tubes were combined and incubated for 15 minutes at room temperature. Then, it was applied to the cells that had been seeded the day before.

In a test tube with PEI-Max, Opti-MEM media and various doses of PEI-Max reagent were placed. In the other tube, Opti-MEM and 200 ng plasmid DNA were added. The two tubes were combined and incubated at room temperature for 30

minutes. It was then applied to the cells that had been seeded the previous day.In the transfection experiments, mEmerald-Vinculin-N-18 (GFP tagged at C-terminus of metavinculin), and mEmerald-N1 (GFP only) plasmids are used. mEmerald-N1 was as a control to compare with metavinculin transfection ratio.

3.2.2.2 Flow cytometry analysis for transfection efficiency and correct dose selection

In order to determine the transfection efficiency, $4x10^4$ cells were seeded into 12-well plate. Next day, cells were transfected with mEmerald-Vinculin-N-18 plasmid. For each day, cells collected with trypsin and centrifuged at 500g for 5 minutes. Then, cells were washed with dPBS and centrifuged at 500g for 5 minutes. Then the cell pellets were dissolved in 400 µl dPBS and transferred into flow tubes. 10.000 cell counts were performed for each condition.

3.2.3 Transfection for focal adhesion observation with confocal microscopy

In order to observe how metavinculin affects cell morphology and focal adhesions at H9C2 cells, cells were seeded into a chambered coverslip with 8 wells for confocal microscopy. The day after, metavinculin plasmid and GFP only plasmid as a control were transfected for Lipofectamine 3000 manufacturer's protocol for 96-well plate.

After 72 hours, cells were observed with confocal microscopy.

3.2.4 Vinculin plasmid cloning from metavinculin plasmid

The plasmid mEmerald-Vinculin-N-18 used in metavinculin experiments contains the mEmerald tag at the C-terminus. The vinculin plasmid was obtained by subcloning since it was not in Addgene where the plasmids were purchased. For this purpose, forward and reverse primers were designed that delete the additional 68 amino acid excess of metavinculin. The designed plasmids were adjusted to 125 ng. The PCR conditions were performed as follows.

Table 5. PCR tube ingredients

Pwo Master	12,5 µl
Forward Primer (10 µM)	1 µl
Reverse Primer (10 µM)	1 µl
Template (mEmeral-Vinculin-N-18)	2 µl
H_2O	8,5 µl
Total	25 µl

Table 6. Thermal cycler conditions

95°C	30 seconds	
95°C	30 seconds	18x
55°C	1 minute	
68°C	10 minutes	
4°C	∞	

0,5 µl of DpnI enzyme at a concentration of 20U/µl was added to the PCR products and incubated for 2 hours at 37°C.

3.2.4.1 Transformation

5 µl of DpnI enzyme digested PCR product was added to 50 µl of DH5α competent cells in which the metavinculin plasmid grew. It was incubated on ice for 30 minutes. After 30 minutes, sample was exposed to heat shock at 42°C for 1 minute. Then 220 µl pre-heated to room temperature LB Broth was added to the sample and it was shaken at 37°C, 250 rpm for 2 hours with environmental shaker. Then sample was seeded to kanamycin agar plate and incubated overnight at 37°C.

3.2.4.2 Plasmid isolation

For the plasmid isolation, colonies were picked with loop and added to tube that contains 5 ml LB Broth and 5 µl kanamycin. Tube was shaken overnight at 37°C to grow.

The day after, plasmid isolation from the colonies was done according to the kit protocol. Obtained plasmid concentration was measured with NanoDrop spectrophotometer. The plasmid was then sent for sequencing to check whether vinculin could be obtained. mEmerald tagged vinculin plasmid was obtained successfully.

3.2.5 Focal adhesion analysis with image j

Image J software was used for quantitative analysis of focal adhesions in H9C2 cells. The analysis steps were carried out as described by Horzum et al. (29). The following steps were applied to the raw confocal microscope fluorescence images:

Firstly, subtract background was applied. Thus, a smooth continuous background was removed from the image. Rolling ball radius is the radius of curvature of the paraboloid was set to 50 pixels. Also sliding paraboloid was selected to turns the rolling ball into a parabolic with a better curvature and the same ball radius in pixels. Then, CLAHE (Contrast Limited Adaptive Histogram Equalization) plugin was applied to improve the image's local contrast. It has 3 options that are block size, histogram bins and maximum slope. In this analysis, block size was 90, histogram bins were 256, the maximum slope was 6 ad no mask and fast. Then, mathematical exponential (exp) was applied to reduce the background and sharpen the image. Brightness/Contrast was adjusted automatically. The image is filtered by the LOG3D (Laplacian of Gaussian or Mexican Hat) plugin using user-defined parameters such as standard deviations in the X, Y, and Z directions. The Z direction is meaningless for 2D images, so slice-by-slice processing is used. The size of the LOG3D filter was set to sigma X=5 and sigma Y=5. Threshold was applied to the resulting gray themed Log image. A grayscale image is transformed to a binary image of black and white using the threshold command. Comparing with the original image, the outline of the cell containing the focal adhesions is drawn in the black and white image. Then, particles were analyzed with analyze particles command. For the choosing of size, pixel minimum and maximum values of focal adhesion areas were checked and 50-1000 pixels were used. Circularity was set to 0.00-0,99 because focal adhesion circularity

can never be 1. At the end of all of these stages, the particle outlines were detected and overlaid on the initial image to visually validate the accurate identification of focal adhesions.

3.2.6 Hypertrophy

For create a hypertrophy model for H9C2 beta adrenergic agonists isoproterenol and phenylephrine was used.

Cells were seeded the day before hypertrophy induction. 10 µM iso and 100 µM pe was applied to the cells.

3.2.6.1 Hypertrophy detection with confocal microscopy

$1x10^4$ cells were seeded with 300 µl volume to chambered coverslip µ-Slide 8 well. After a day, cells were treated 10 µM iso or 100 µM pe. After 48 hours, cells were fixed with 4% PFA. Briefly, cold 4% PFA were applied on cells and incubated 15 minutes at room temperature. Then wells were washed with dPBS 3 times.

After fixation, cells were stained with 1:20 diluted Alexa Fluor 488 phalloidin (6,6 µM) to stain F-actin of cells. With dye, cells were incubated 15 minutes at room temperature. Then, wells were washed with dPBS once and images were taken with confocal microscopy.

3.2.6.2 Hypertrophy detection with flow cytometry

In order to check the hypertrophy efficiency, $3x10^4$ cells were seeded into 12-well plate. The day after, cells were treated with iso and pe with different doses. For each day, cells collected with trypsin and centrifuged at 500xg for 5 minutes. Then, cells were washed with dPBS and centrifuged at 500xg for 5 minutes. Then the cell pellets were dissolved in 400 µl dPBS and transferred into flow tubes. Then, flow cytometry experiment was performed for 3-4 days.

3.2.7 Protein isolation

Cell lysates were pipetting with 1x RIPA includes PI and PMSF and incubated 10 minutes on ice. Then, cells were pipetting and incubated on ice extra 10 minutes. Finally, cells were centrifuged at 14.000 G for 10 minutes at 4°C. Supernatant proteins were transferred to the new tubes and stored at -80°C.

3.2.8 Qualifying of protein concentration

Protein concentration qualified with Bradford Assay method. Protein concentrations were compared with BSA protein concentration graphic. Firstly, BSA were used as standards with 1, 2, 4, 6, 10 µg/µl. 1,2, and 4 µl of each protein sample was also used. 1,2,4 µl of dH2O was used as a blank. In a 96 well plate, BSA standards and protein samples were put and 200 µl of Bradford assay were added on the proteins. 96 well plate was read at 595 nm absorbance after the 5 minutes of incubation at dark.

Blank results were averaged and subtracted from proteins' absorbance values. For the BSA standard results, a line graph was drawn. Protein concentration of samples were calculated to the line equation of the BSA standards.

3.2.9 Western blot

5x Laemmli sample buffer was diluted to 1x with 25 µg of protein samples and tube volume was completed to 20 µl with dH_2O. Then, tubes were boiled at 95°C for 5 minutes and they were put in the ice and centrifuged maximum speed for 1 minutes.

Protein samples were loaded on the gel. 12,5% of SDS-PAGE gel were used for smaller kDa of proteins. 8% of SDS-PAGE gel were used for highest kDa of proteins.

Samples were run at 60V till the proteins were passed the separating gel. Then, they were run at 120V till the at the end of the gel.

12,5% gels were transferred to 0,2 μm pore sized nitrocellulose membrane for 50 minutes and 8% gels were transferred to the 0,45 μm pore sized nitrocellulose membrane for 60 minutes in the Bio-Rad trans-blot semi dry system. Before the transfer, filter papers and nitrocellulose membrane were incubated in 1x transfer buffer for 5 minutes.

After transfer, gels were stained with Coomassie brilliant blue to checking of the transfer success. After the gel was stained, gel was incubated in destaining solution to remove the dye from the gel and see the proteins. The membrane was blocked with 5% skimmed milk for an hour at room temperature. Then, membrane was cut according to related protein kDa. Each membrane was incubated with related primary antibody at 4°C overnight.

The next day, primary antibodies were collected and membranes were washed with 1x PBST for 3 times along 10 minutes at room temperature. Then, membranes were incubated with peroxidase-conjugated anti-rabbit or anti-mouse 1:5000 secondary antibody for an hour at room temperature. After that, membranes were washed with 1x PBST for 2 times along 10 minutes and 1x PBS for 1 time along 10 minutes. Finally, chemiluminescent reagent was applied and incubated in the dark for 2-3 minutes. The images were obtained in the ChemiDoc image analyzer and results were analyzed using Image Lab software.

3.2.9.1 Western blot for focal adhesion detection

Pimary antibodies used for focal adhesion detection are α-Actinin rabbit monoclonal antibody (1:2000), FAK rabbit antibody (1:2000), Talin-1 rabbit monoclonal antibody (1:2000), Vinculin rabbit antibody (1:2000). β-Actin mouse monoclonal antibody (1:10000) was used as a housekeeping protein. Then, anti-rabbit IgG, HRP-linked Antibody (1:5000) was used as a secondary antibody.

3.2.9.2 Western blot for hypertrophy detection

Pimary antibodies of α-Actinin rabbit monoclonal antibody (1:2000), FAK rabbit antibody (1:2000), Talin-1 rabbit monoclonal antibody (1:2000), Vinculin rabbit antibody (1:2000) was used in hypertrophy conditions. Also, GAPDH monoclonal antibody (1:3000) was used as a housekeeping protein since β-Actin could not be used because it is affected by hypertrophy induction. Then, anti-mouse IgG, HRP-linked antibody (1:5000) was used.

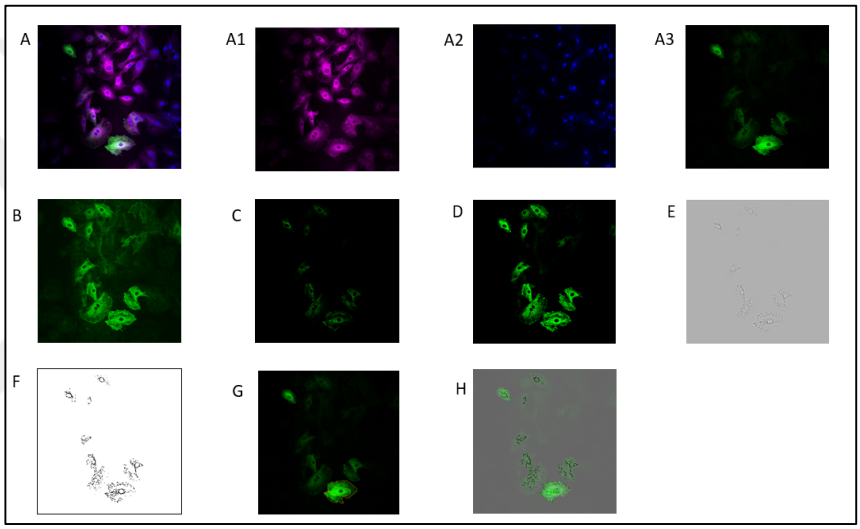

Figure 9. Confocal image analysis steps with image j.

Image A is a raw data image in czi format taken with confocal. First, when opening the image with Image J, the split channel was selected and the cell mask channel (A1), which stains the cell membrane, was separated from the NucBlue channel (A2), which stained the cell nucleus, and the gfp channel (A3), which showed transfection.

Analysis was performed via the GFP channel in A3 Image. First of all, the subtract background command was selected from the process part (B). This command clears the unevenly lit background for a more robust analysis. This command uses sliding paraboloid or Radius ball. The rolling ball radius should at least be set to the size of the largest object that is not part of the background. The generally preferred 50 were selected in this analysis.

Local contrast was enhanced using Contrast Limited Adaptive Histogram Equalization (CLAHE) plugins (B). This command contains 3 parameters, these are block size, histogram bins and maximum slope. Block size is the size of the local region around a pixel to which the histogram is equalized. In this analysis, block size 90 was made. histogram bins; It is the number of boxes used when synchronizing the histogram. Since it works in byte units, more than 256 is meaningless. In this analysis, histogram bins 256 was chosen. 1 original image on maximum slope. Limits the contrast stretch. 6 were selected in this analysis. Mask and fast were not used.

Then the mathematical Exp command was applied to minimize the background (C).

As the whole image faded, Brightness & contrast was adjusted automatically and cells were allowed to be seen (D).

Laplacian of Gaussian Log3D plugins applies a Laplacian of Gaussian (Mexican Hat) filter to a 2D image. It is used to detect objects, set boundaries and extract features. By running this plugin, the standard deviation is limited to x, y, z dimensions. Since there is no z dimension, only x and y 5 are selected. The boundaries of the cell have been determined (E). Since the new gray themed image is 32-bit, it was converted to 8-bit before proceeding to the next stage. Threshold command does not work for 32-bit image.

With the Threshold command, the gray themed log image is converted to a binary image. Blacks are set to 1 and white background to 0 (F).

Then the original raw data image is opened and the main image and the thresholded image are synchronized by choosing synchronize Windows. The periphery of the cell was carefully drawn so that the nucleus of the cell was out. 50-1000 was selected for you with the analyze particles command on the thresholded image. Circularity was chosen between 0-0.99. Since focal adhesions cannot be round

due to their structure, the upper limit of circularity 0.99 was chosen. Focal adhesion area information was obtained (G).

4 RESULTS

The H9C2 cell line was initially derived from embryonic rat ventricular tissue which is critical as cardiac hypertrophy coming about from hypertension primarily happens within the ventricular muscle of the heart. In spite of the fact that H9C2 cells are not able to beat, they still share some similar features with primary cardiomyocytes, including membrane morphology and electrophysiological attributes. More importantly, they can show hypertrophy-associated characteristics when stimulated with hypertrophic agents in vitro (30). For all these reasons, H9C2 cells were selected for the purpose of the project and experiments were carried out with this cell line.

4.1 Optimizing the Transfection Efficiency With H9C2

To understand the role and importance of vinculin and its isoform metavinculin in heart tissue and to observe their changes in hypertrophy state, these genes were upregulated in cardiac muscle cell by transfection. To do this, cationic lipid agents called Lipofectamine 3000 and PEI-MAX were tried. In order to understand which agent transfects the H9C2 cell line more efficiently, Lipofectamine 3000 and PEI-MAX were applied at different doses and the cells were observed with a fluorescent microscope day by day. Highest transfection yields were obtained at the 72nd hour of transfection when the plasmids were applied with lipofectamine 3000 at a ratio of 1:1 (lipofectamine: plasmid). Since the yield of Pei-Max was really low, the experiments throught this thesis were performed with lipofectamine transfection agent for H9C2 cells.

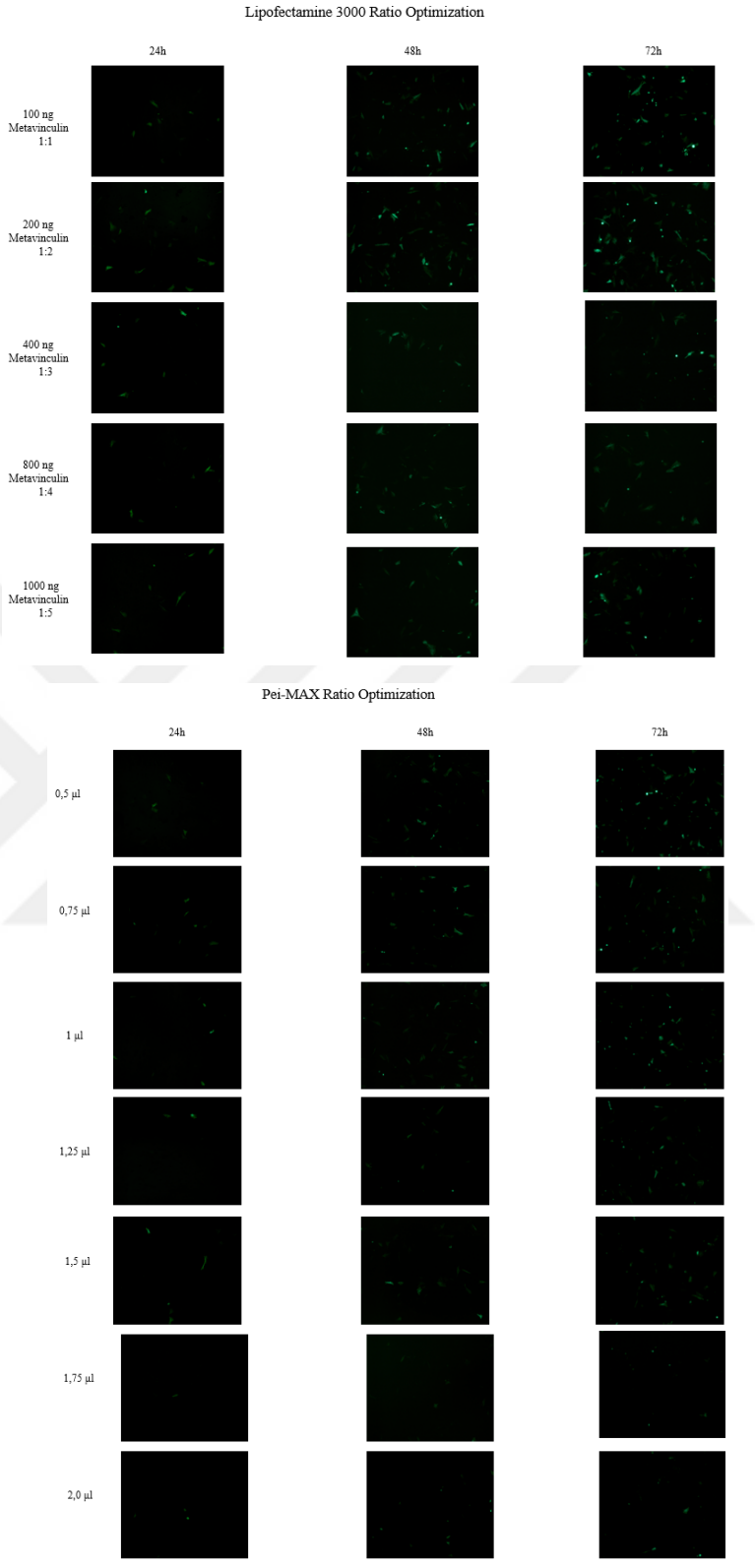

Figure 10. Transfection optimization for H9C2 cells via fluorescent microscope

H9C2 cells were transfected with lipofectamine 3000 as 200 ng to 1000 ng metavinculin plasmid and with PEI-Max 0,5 to 2 µl and 200 ng plasmid. Images were obtained with fluorescent microscope 10x magnification. It was seen that the transfection efficiency at the day 3 with 1:1 plasmid: lipofectamine 3000 ratio was the best result.

4.2 Flow Cytometry Analysis for Transfection Efficiency

Flow cytometry assay was performed to determine the most efficient dose and time and percentage of transfection for H9C2 cells in order to correlate the results visually observed with a fluorescent microscope on a numerical data (Fig. 11). For this purpose, flow cytometry test was performed on cells transfected with GFP conjugated metavinculin plasmid by first observing with a fluorescent microscope at the 72nd hour when brightness and vitality were highest. Then, after it was decided that the cells transfected with metavinculin were sufficient in terms of viability and brightness in the fluorescent microscope, flow cytometry experiment was performed.Untransfected cells were used as the control group. First, control group cells were measured with forward scatter (FSC) and side scatter (SSC) graphics. Thus, the viable cell population was plotted. (Fig. 12).

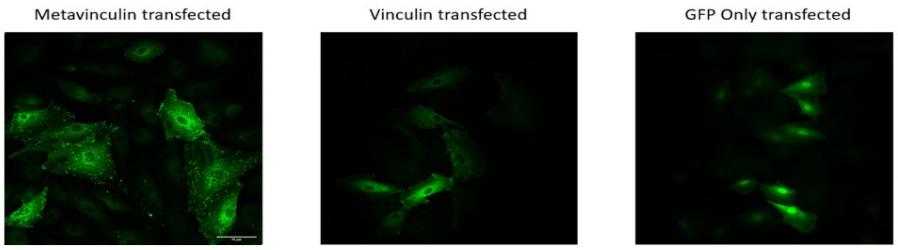

Figure 11. Cell morphology of transfected H9C2 cells.

(Cells were transfected and imaged with Confocal Microscopy at 20x magnification to compare cell morphologies)

A flow cytometry experiment was performed to measure the efficiency of transfection in H9C2 cells. At 72nd hours of transfection, cells were analyzed by forward and side scattering using flow cytometry. In this way, the population was

selected according to the viability of the cells. In addition, fluorescent channel and cell count plots were used to understand the transfection efficiency according to green fluorescent protein (GFP) fluorescence intensity. It was determined that the closed population had 78.76% fluorescence intensity.

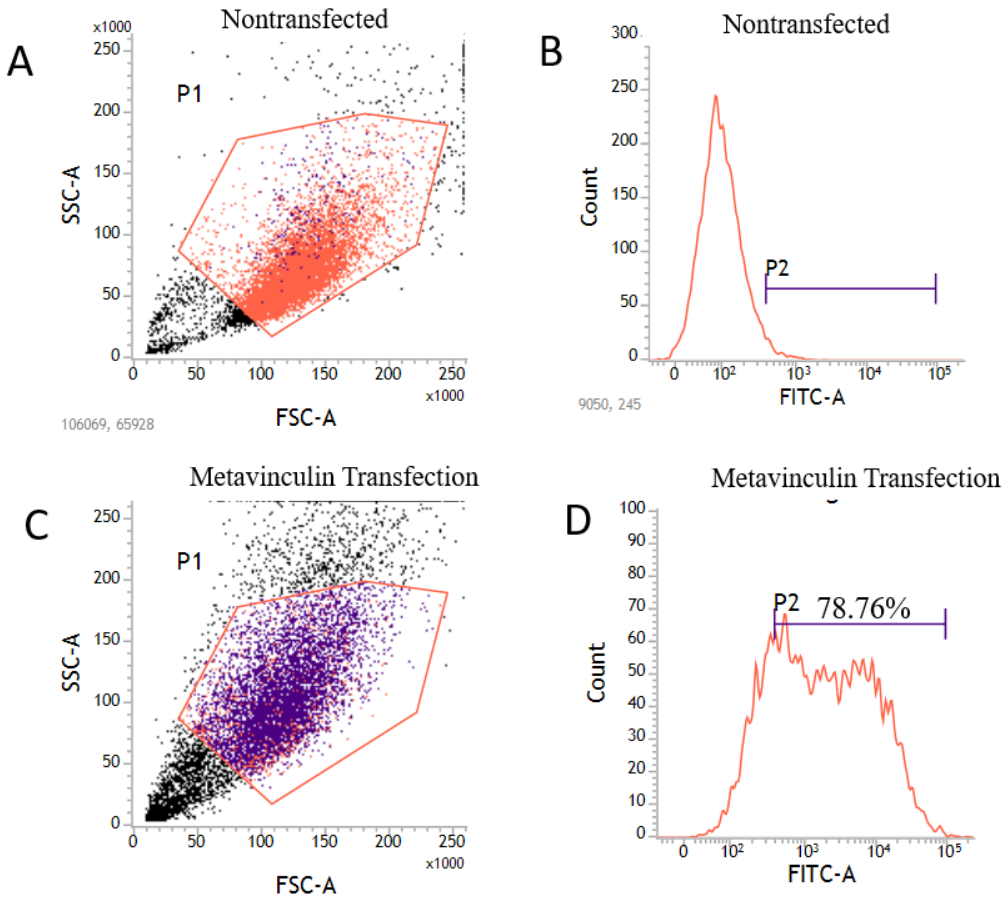

Figure 12. Flow cytometry analysis for transfection efficiency

(100 ng mEmerald-Vinculin-N-18 (metavinculin) plasmid was transfected for H9C2 with lipofectamine 3000. At the day 3, when transfection fluorescent ratio was maximum, flow cytometry experiment was performed. Transfection efficiency was visually inspected before flow cytometry and was performed when the yield was between 60% and 70%. The experiment was not performed when the transfection efficiency was observed below this ratio. Control cells were not transfected. Population was gated by forward and side scatter graph and FITC green fluorescent detection laser graph was shown for H9C2. Percentages of gated cells were represented on the figure. It was observed that transfection efficiency was 78.76% in the transfected group in the selected populations on day 3.)

4.3 Transfected Cell Analysis for Focal Adhesion Observation

Both MVcl and Vcl are known to be localized to FAs which are essential for biological processes including the maintenance of cell shape, motility, tissue structure, and proliferation. Since the expression of vinculin isoforms can influence the response of cardiomyocytes to hypertrophy, we attempted to find a link between the area of focal adhesions and the expression of these proteins. We found that there were no statistical difference between the calculated mean areas of focal adhesions of MVcl and Vcl-transfected cells (Fig. 13-16). However, the MVcl-transfected cells had statistically higher surface area compared to Vcl-transfected cells (Fig. 17).

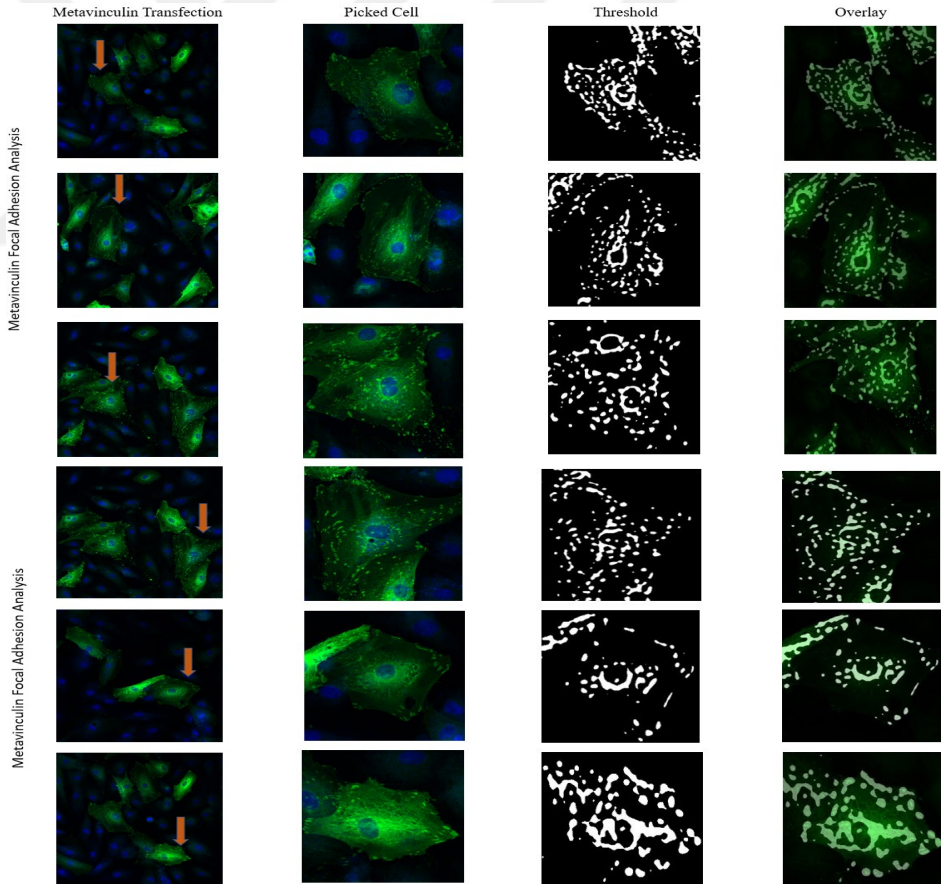

Figure 13. Focal adhesion analysis of metavinculin transfected H9C2 cells.

(Images of metavinculin transfected H9C2 cells were obtained by confocal microscope. These images were analyzed for focal adhesions with ImageJ software as described by Horzum et al. In the figure, the confocal image of the cell, the selected cell for analysis, the binary image with two-pixel values (Log) image, and the focal adhesions merged on the major image are shown respectively)

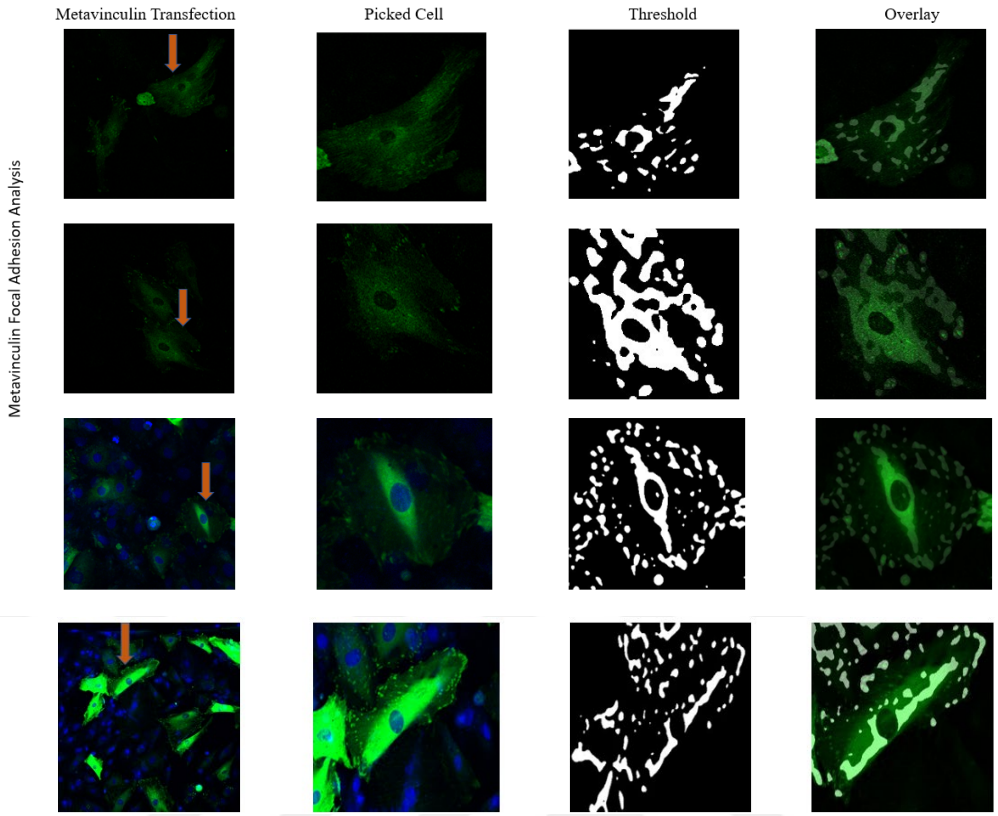

Figure 13. Focal adhesion analysis of metavinculin transfected H9C2 cells. (continued).

(Images of metavinculin transfected H9C2 cells were obtained by confocal microscope. These images were analyzed for focal adhesions with ImageJ software as described by Horzum et al. In the figure, the confocal image of the cell, the selected cell for analysis, the binary image with two-pixel values (Log) image, and the focal adhesions merged on the major image are shown respectively. Ten independent cells were analyzed in the metavinculin transfected cell group)

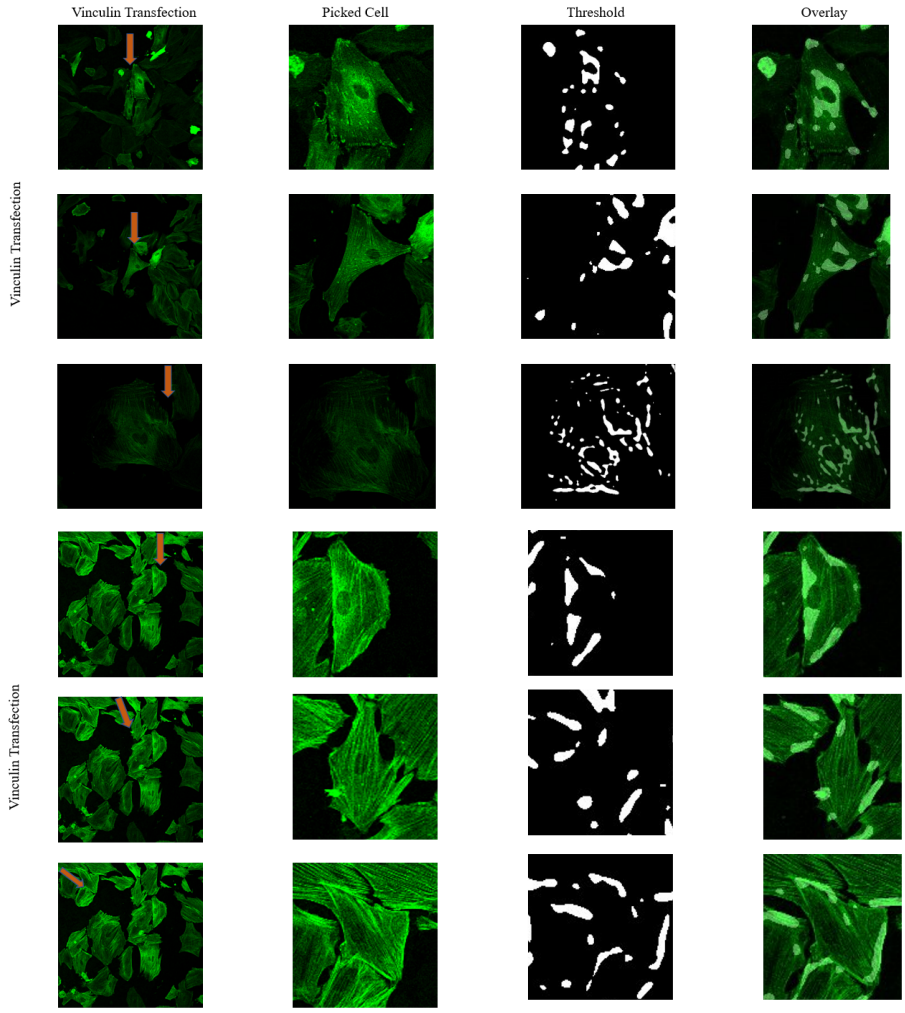

Figure 14. Focal adhesion analysis of vinculin transfected H9C2 cells.

(Images of metavinculin transfected H9C2 cells were obtained by confocal microscope. These images were analyzed for focal adhesions with ImageJ software as described by Horzum et al. In the figure, the confocal image of the cell, the selected cell for analysis, the binary image with two-pixel values (Log) image, and the focal adhesions merged on the major image are shown respectively)

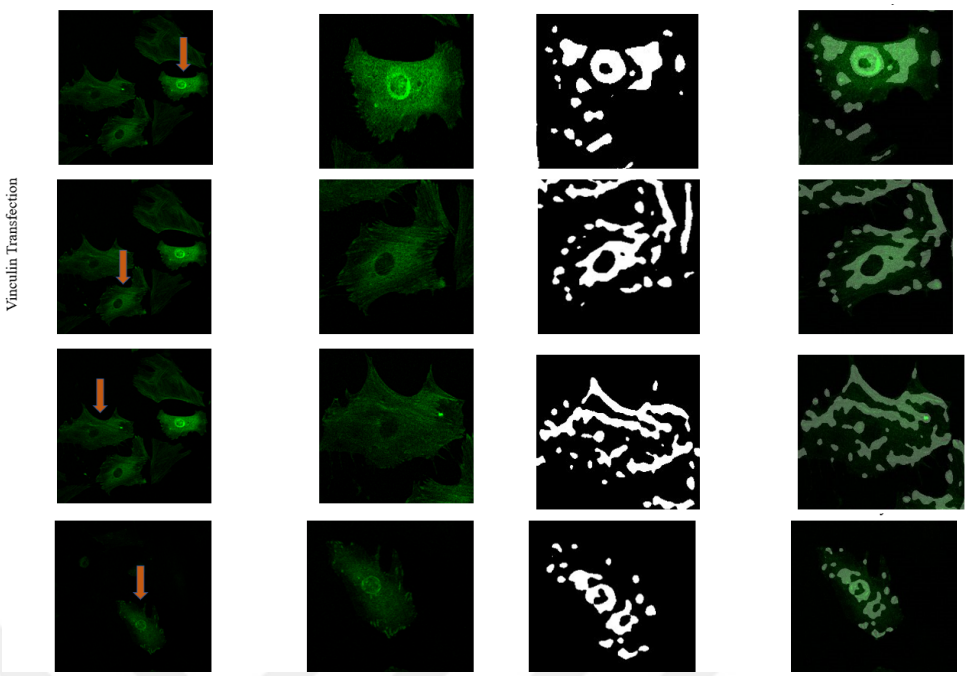

Figure 14. Focal adhesion analysis of vinculin transfected H9C2 cells (continued).

(Images of vinculin transfected H9C2 cells were obtained by confocal microscope. These images were analyzed for focal adhesions with ImageJ software as described by Horzum et al. In the figure, the confocal image of the cell, the selected cell for analysis, the binary image with two-pixel values (Log) image, and the focal adhesions merged on the major image are shown respectively. Ten independent cells were analyzed in the vinculin transfected cell group)

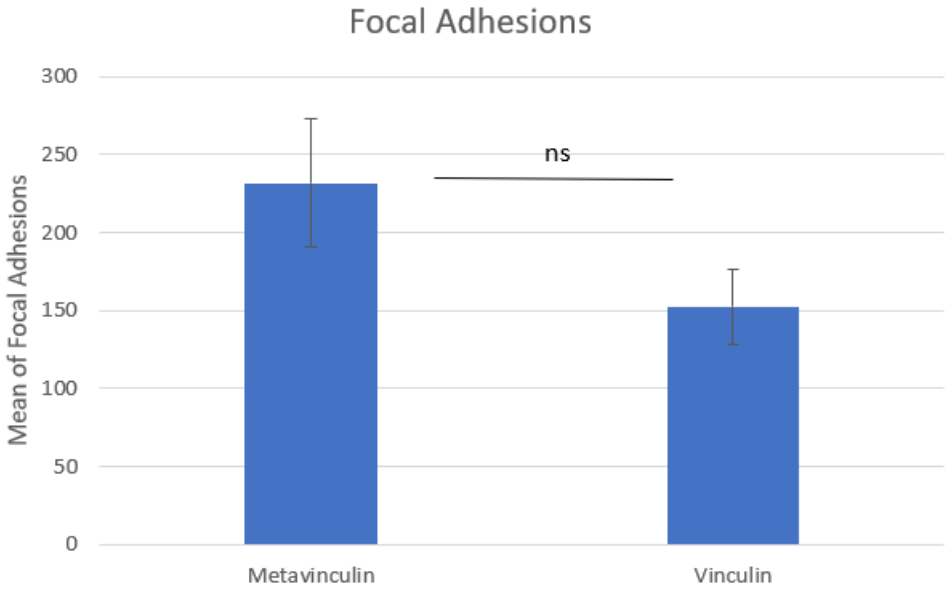

Figure 15. Comparison of metavinculin vs vinculin focal adhesions.

(Analyzed cells were demonstrated as histogram in the figure. Bar graph represents n=10 independent cells as mean and standard error (ns $p>0.05$, *$p < 0.05$, **$p < 0.01$, ***$p < 0.001$))

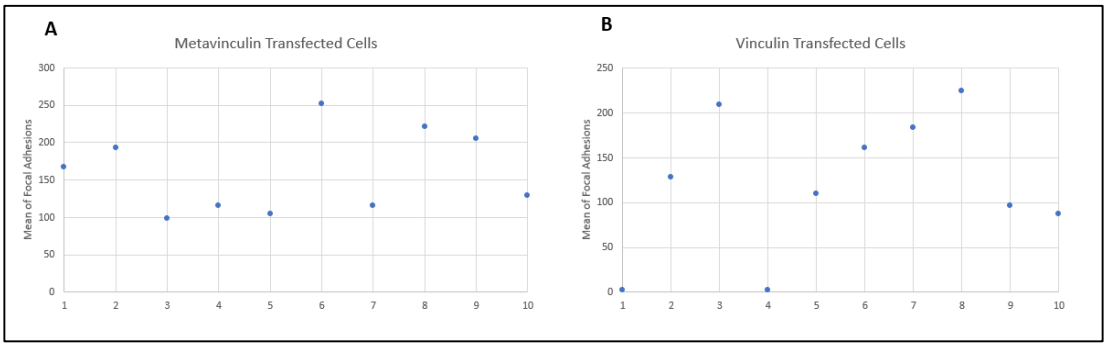

Figure 16. Graph of focal adhesions per cell.

(The mean distribution of focal adhesion area of 10 independent cells analyzed for each condition is shown)

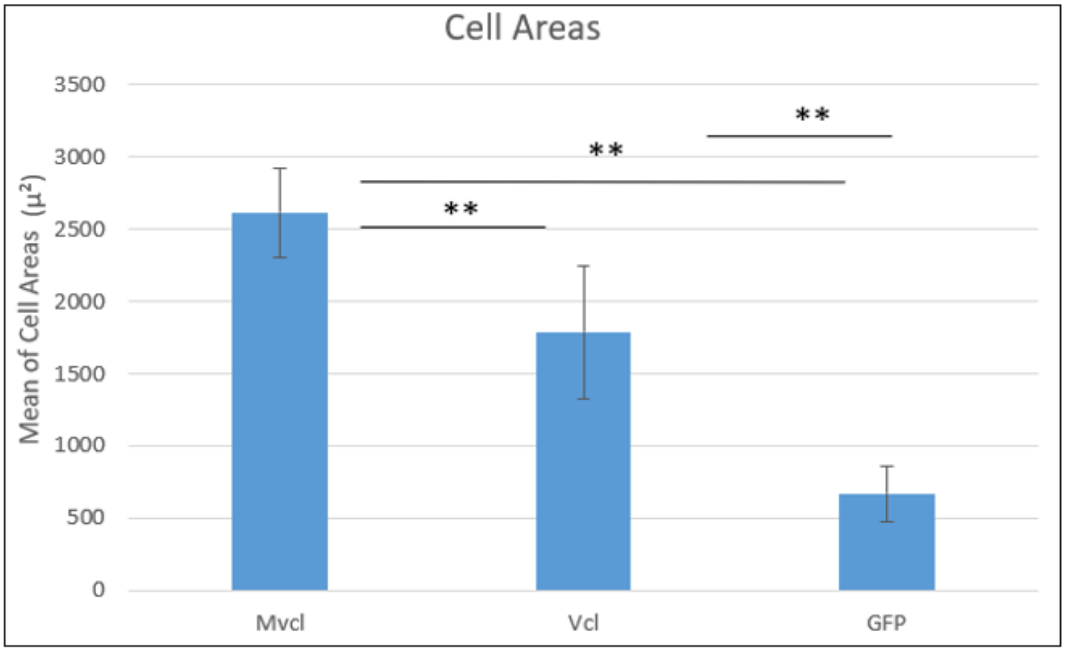

Figure 17. Cell areas comparison of transfected H9C2 cells.

(H9C2 cells transfected with MVcl, Vcl and Only GFP plasmids were area measured with Image J. Bar graph represents n=10 independent cells as mean and standard error (ns p>0,05, *p < 0,05, **p < 0,01, ***p < 0,001))

4.4 Induction and Detection of Hypertrophy in H9C2 Cells

Cardiac hypertrophy is a response of the heart to adapt to pressure or volume stress, mutations of sarcomeric (or other) proteins. H9C2 cells were treated with hypertrophy-stimulating agents isoproterenol and phenylephrine to mimic this response and create a hypertrophy model. The dose dependence of hypertrophy induction was first followed by fluorescence imaging with Alexa Fluor 488 phalloidin or rhodamine phalloidin that labels F-actin (Fig. 18-20). Consistent with the literature, upon induction with 10 μM isoproterenol and 200 μM phenylephrine H9C2 cells had altered microfilament organization indicative of hypertrophy.

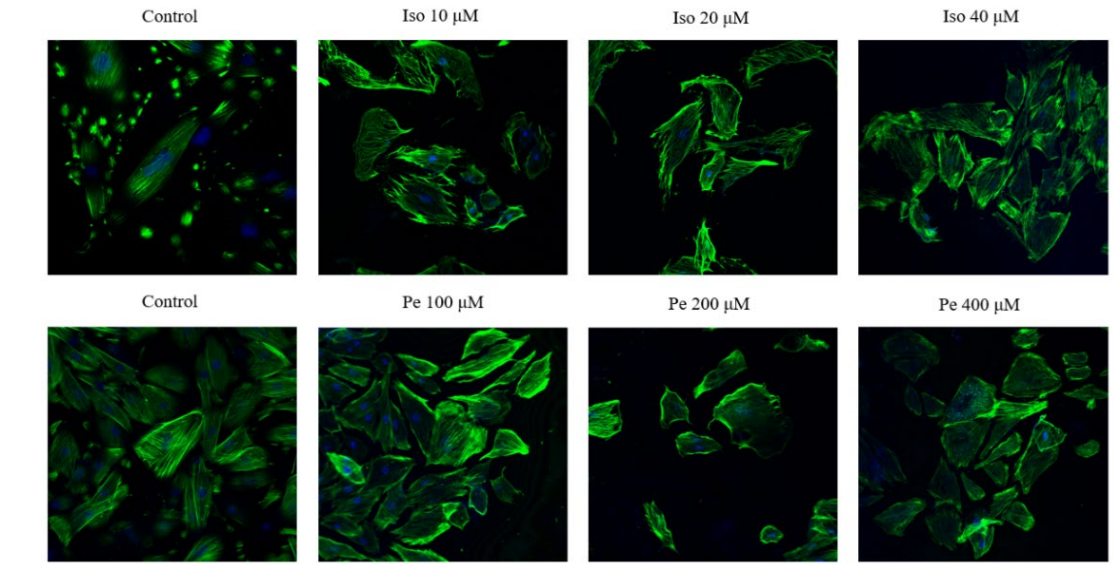

Figure 18. Confocal image of hypertrophy induced H9C2 cells.

(H9C2 cells were hypertrophy induced by different doses of iso and pe. Alexa Fluor 488 phalloidin were used to stain F-actin. NucBlue counterstain was used to stain nucleus of cells. Cells were imaged 20x magnification. While regular F-actin was observed in control cells, it was observed that F-actin fibrils were disrupted in case of hypertrophy)

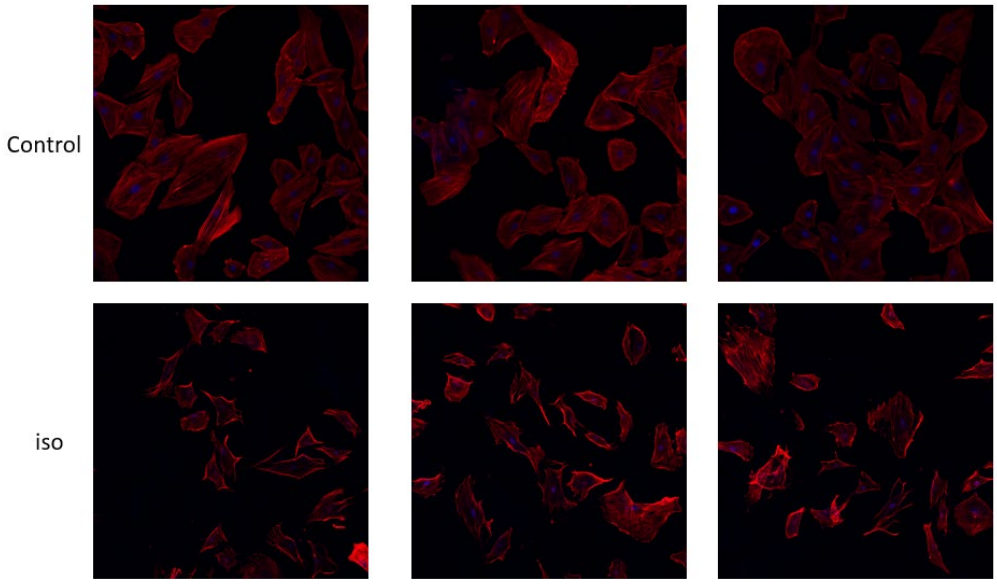

(A)

(20x image of isoproterenol-induced hypertrophic cells stained with Rhodamine phalloidin and NucBlue to observe F-actin fibrils disruption)

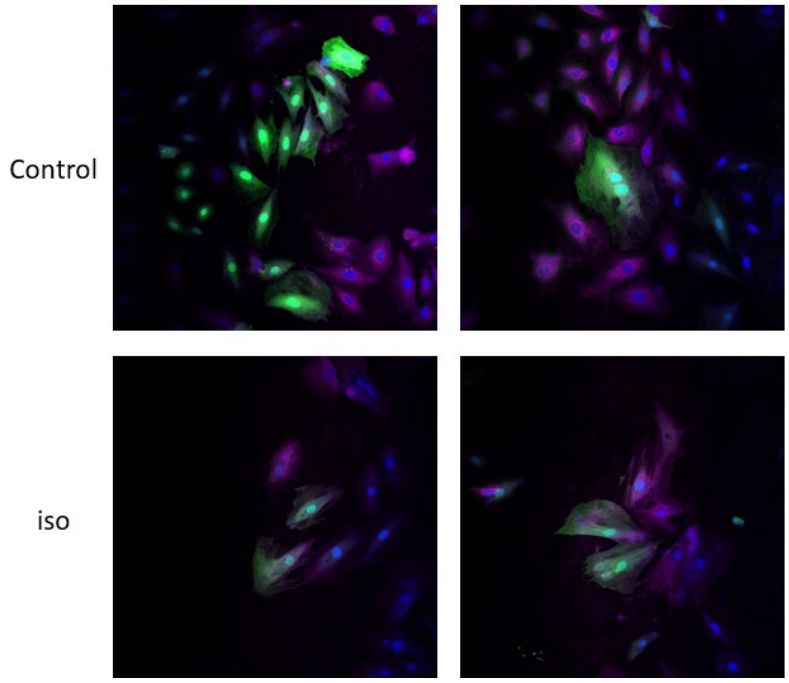

(B)

Figure 19. A) Confocal image of isoproterenol induced H9C2 cells (rhodamine). B) Confocal image of isoproterenol induced H9C2 cells (cellmask).

(20x image stained with CellMask staining the plasma membrane of isoproterenol-induced H9C2 hypertrophic cells transfected with GFP Only plasmid)

In addition to fluorescence imaging, hypertrophy induction in H9C2 cells were followed by flow cytometry (Fig. 20). We observed that FSC which is a measure of cell size increased even at the lowest doses of isoproterenol and phenylephrine starting within 24 hrs of treatment.

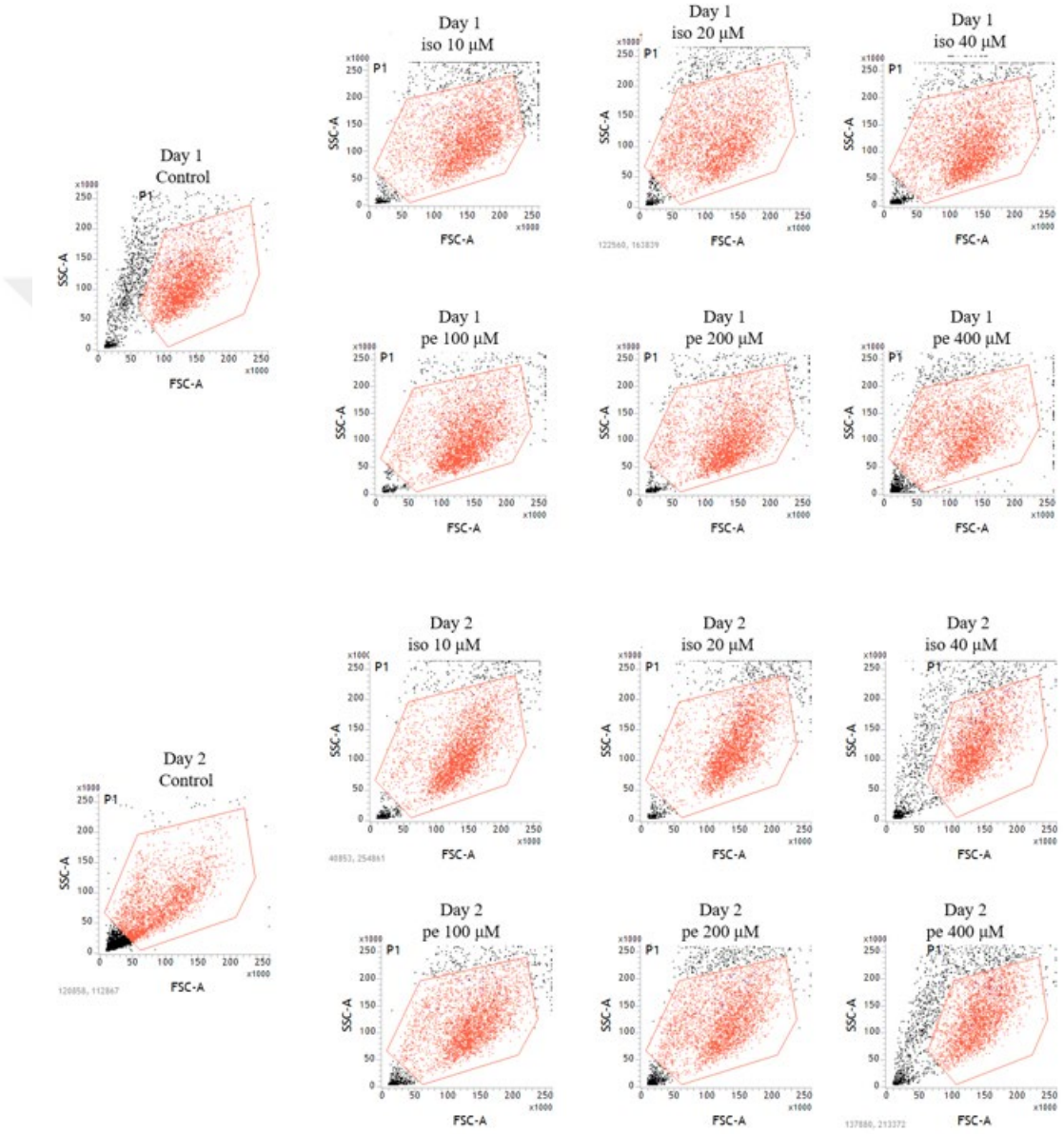

Figure 20. Hypertrophy detection with flow cytometry.

(Different doses of iso and pe was used to create hypertrophy on H9C2 cells. At the day 1 and 2, flow cytometry experiment was performed. Control cells were not hypertrophied. Population was gated by forward and side scatter graph was shown for H9C2. It was observed that hypertrophy was occurred efficiently on day 2. n=3 conditions were performed)

4.5 Effect of Metavinculin Expression on the Mean Focal Adhesion Areas of Hypertrophy Induced H9C2 Cells

MVcl expression is reduced in cultured primary cardiomyocytes suggesting a link between the expression levels of this vinculin isoform with force generation (31). Therefore, we hypothesized that the morphology of focal adhesions may be different in MVcl expressing cells compared to only Vcl expressing cells that were induced to hypertrophic state. Although the areas of focal adhesions were higher in MVcl expressing cells, the observed difference was not statistically significant from hypertrophic cells expressing Vcl only (Fig. 21, 22, and 23). However, the calculated surface areas for both MVcl and Vcl expressing cells were similar during hypertrophy (Fig. 24)

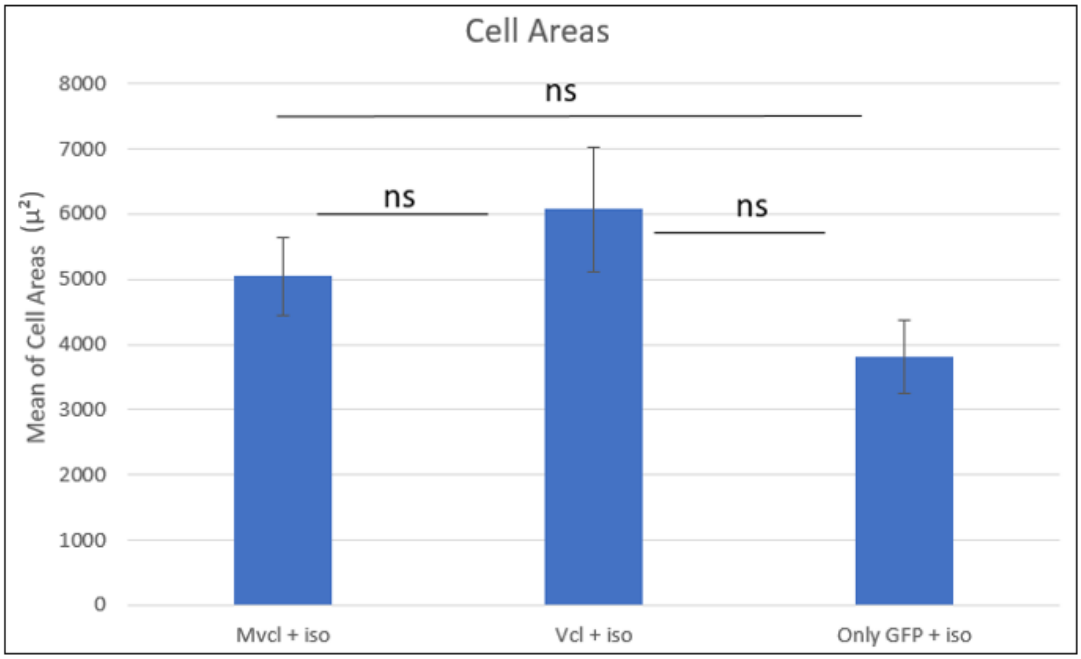

Figure 21. Comparison of metavinculin and vinculin transfected hypertrophic cells focal adhesions.

(Analyzed cells were demonstrated as histogram in the figure. Bar graph represents n=10 independent cells as mean and standard error (ns p>0,05, *p < 0,05, **p < 0,01, ***p < 0,001))

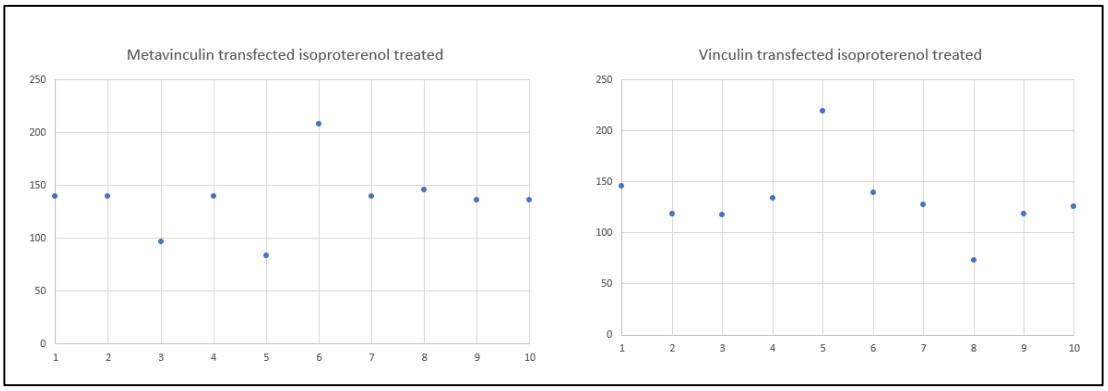

Figure 22. Graph of focal adhesions per cell.

(The mean distribution of focal adhesion area of 10 cells analyzed for each condition is shown)

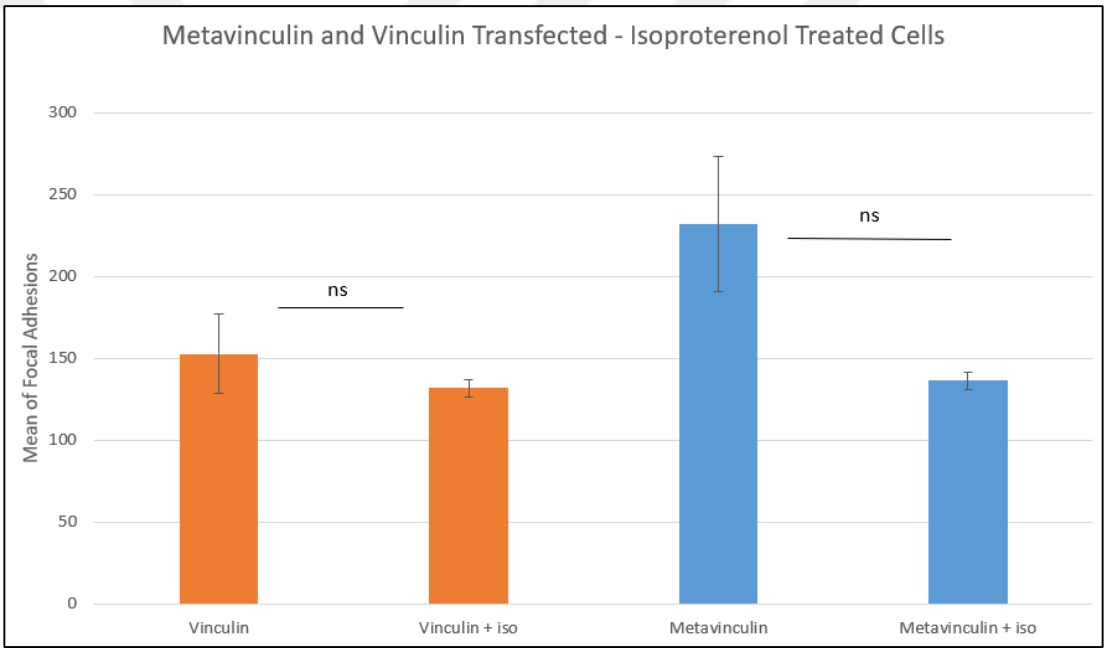

Figure 23. Focal adhesion comparison plot of MVcl and Vcl-transfected H9C2 cells and their hypertrophied state.

(The mean distribution of focal adhesion area of 10 cells analyzed for each condition is shown. Bar graph represents n=10 independent cells as mean and standard error (ns $p>0.05$)

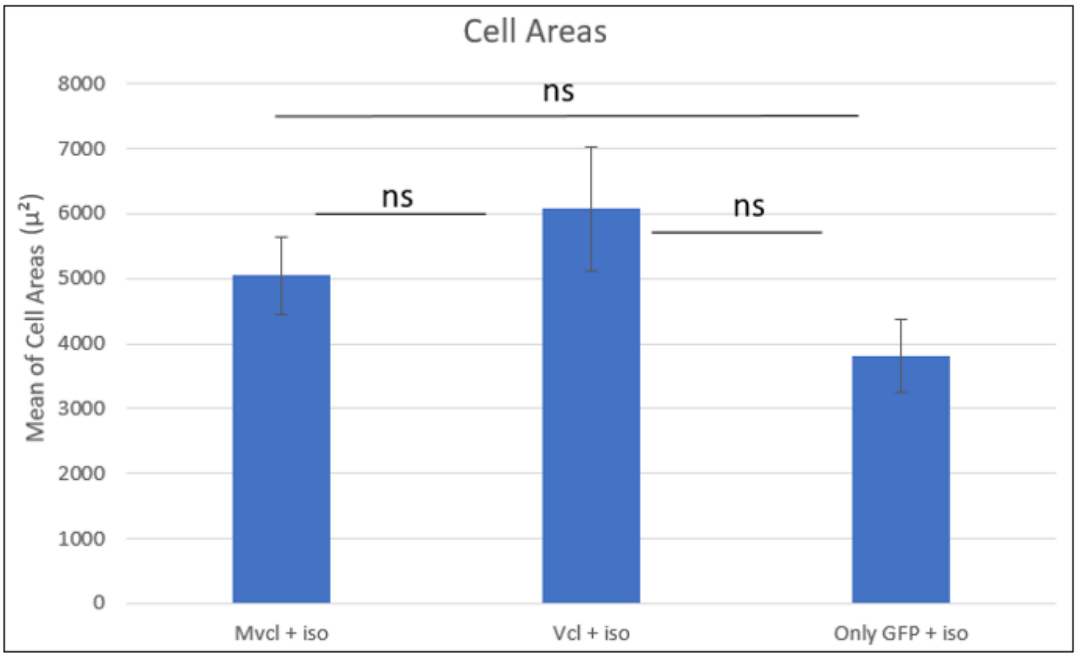

Figure 24. Cell areas of transfected-hypertrophied H9C2 cells.

(The mean distribution of cell area of n=10 cells analyzed for each condition is shown. Bar graph represents 3 independent repeats as mean and standard error (ns p>0,05)

4.6 Western-Blot Analysis of Focal Adhesion Proteins

An increase in MVcl expression may alter the protein profile of other well known focal adhesion proteins and vinculin binding partners including focal adhesion kinase (FAK) (125 kDa), Talin-1 (270 kDa), and α-Actinin (100 kDa). Therefore, to check the vinculin and metavinculin effect on the levels of focal adhesion proteins we performed western blot analysis. According to our results we found no significant differences between control and vinculin isoform expressing cells in terms of focal adhesion protein levels (Fig. 25). Also, FAK, Talin-1, -actinin, and vinculin, all of which have been linked to hypertrophy, were examined at the protein level as well. (Fig. 26)

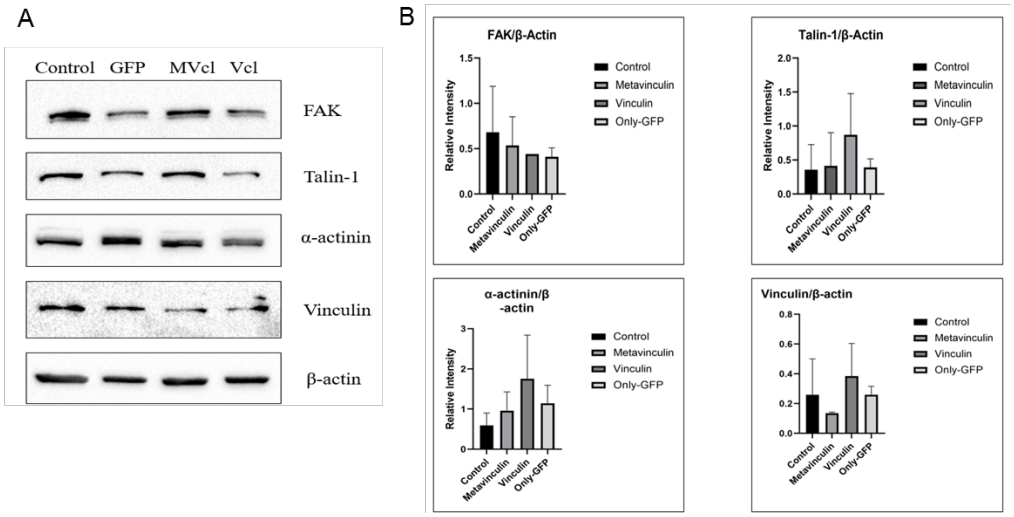

Figure 25. Effect of vinculin and metavinculin transfection on focal adhesion proteins in cardiomyocyte.

((A) Western Blots of transfected cells. Cells were collected and lysed at the 72nd hour of transfection. Proteins were run 8% SDS-PAGE for FAK and Talin-1, 12,5% SDS-PAGE for α-actinin and vinculin. β-actin were used for housekeeping protein. Protein band analyses were performed with Image Lab software. 4 independent experiments were performed (B) Bar graph demonstrates the normalized protein/β-actin ratio for control, MVcl transfected, Vcl transfected and GFP only transfected H9C2 cells. 4 independent experiments were represented as mean and standard deviation in the bar graph)

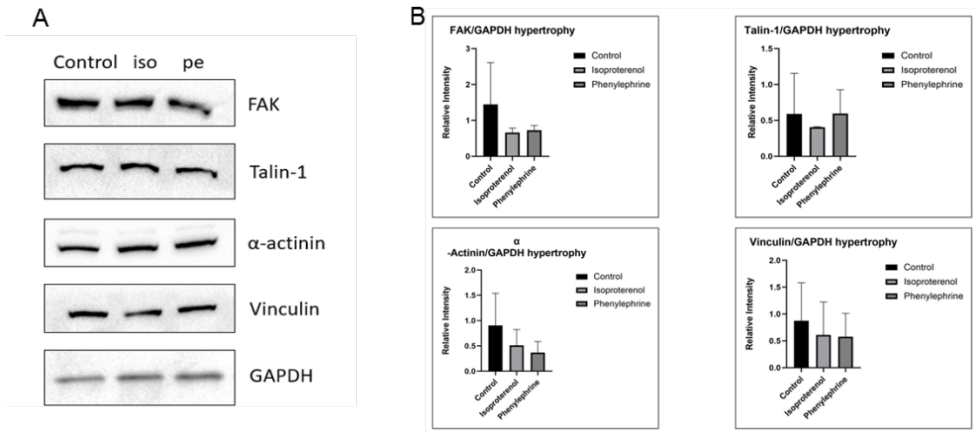

Figure 26. Effect of hypertrophy on focal adhesion proteins in cardiomyocyte cells.

((A) Western Blots of hypertrophied cells that were collected and lysed at the 48th hour of treatment. Proteins were run 8% SDS-PAGE for FAK and Talin-1, 12,5% SDS-PAGE for α-actinin and vinculin. GAPDH were used for housekeeping protein. (B)Protein band analyses were performed with Image Lab software. Four independent experiments were performed. BHypertrophic cells were collected and lysed 48th hour. Proteins were run 8% SDS-PAGE for FAK and Talin-1, 12,5% SDS-PAGE for α-actinin and vinculin. GAPDH were used for housekeeping protein because of β-actin is affected from hypertrophy. Protein band analyses were performed with ImageLab software. Focal adhesion proteins were compared to GAPDH with normalization. Bar graph demonstrates the normalized protein/GAPDH ratio for control, hypertrophied by iso, and hypertrophied by pe H9C2 cells. Four independent experiments were represented as mean and standard deviation in the bar graph)

5 DISCUSSION

Vcl is a membrane-related protein that binds focal adhesions, adherent junctions, and costameres to the actin cytoskeleton by binding to F-actin, α-actinin, α-catenin and talin. In cardiomyocytes, Vcl is located in the lateral sarcolemma, costameres, and intercalated discs. The latter are special cardiac muscle connections transmitting contractile forces (4). Mutations in the insert region of metavinculin, the muscle-specific isoform of vinculin, have been linked to cardiomyopathy. Therefore, our main goal in this project was to investigate how metavinculin affects the actin cytoskeleton, focal adhesions, and the hypertrophic response of H9C2 cells.

Vinculin is involved in the stabilization of focal adhesions and transmission of extracellular mechanical stimuli to the cytoskeleton via integrins (32). Zemljic-Harpf et al. found reduced (60 percent) expression of vinculin and metavinculin in Vcl +/- mice, as well as aberrant electrocardiograms and intercalated disks. While cardiac functions were normal, acute hemodynamic stress caused Z-lines to become misaligned, resulting in aberrant myocardial ultrastructure. These findings suggest that vinculin/metavinculin expression is critical for myocyte shape, particularly under stress (4).

In this study, we used the H9C2 cell line, a subclone of embryonic BD1X rat heart tissue that exhibits many skeletal muscle characteristics. These cardiac myoblasts can be used to investigate the cellular and molecular changes that occur as a result of the hypertrophic reaction (33). Within the scope of these studies, an increase in cell size, accumulation and rearrangement of contractile proteins, and up-regulation of the hypertrophy-specific gene profile can be examined.

FAs, made up of more than a hundred proteins, are linked to the cytoskeleton and serve a variety of functions assisting the physical contact between the inside and outside of a cell . As a result, understanding fundamental biological processes such as cell shape, motility, tissue structure, proliferation, and differentiation necessitates quantitative analysis of FAs. Because cells can generate a large number of micrometer-

scale FAs, quantitative examination of these structures requires targeted image analysis techniques (29). Depending on the FA's maturation stage and cell type, focal adhesions can range in size from 0.25 to 10 um. Focal adhesions can be detected by identifying a protein of interest residing in these complexes. Because both vinculin and metavinculin are one of these proteins, we were able to assess the regions of focal adhesions using the transient transfection of GFP-tagged vinculin isoforms under a variety of conditions.

Firstly, the transient transfections in H9C2 cells were optimized using different transfection agents. In summary, the optimization experiments for transfections were done by testing lipofectamine 3000 (a cationic lipid) and polyethylenimine (PEI-Max; a steady cationic polymer) agents at different ratios (34). While both reagents are reportedly facilitate the foreign DNA uptake by endocytosis, transfection yield obtained for H9C2 cells were higher for Lipofectamine 3000 as qualitatively assessed by fluorescence microscopy. Next, the quantitative measurement of transfection efficiency was performed by flow cytometry assay to determine the most efficient dose and time points for H9C2 cells under our experimental conditions. When the manufacturer's protocol was applied with Lipofectamine 3000, highest fluorescent intensity was detected at 48-72 hours post-transfection. These transfection conditions were used in the functional experiments of this thesis.

Initially, the effect of muscle specific metavinculin expression in H9C2 cells were examined by measuring cell size, focal adhesion area and general cellular morphology. As a control, we used vinculin expressing cells since this protein is endogeneouly present in H9C2 cell line (Figure 25). We observed that MVcl-GFP and Vcl-GFP expressing cells had a larger surface area compared to cells transfected with only GFP (Figure 11 and 17) while the area of MVcl-GFP expressing cells were highest (Figure 17). Also, we measured the focal adhesion areas for these cells and found that cells transfected with metavinculin had more FAs. Although, our results were not statistically significant from Vcl-GFP expressing cells, it is consistent with the previous observations by Lee et al. showing a higher surface area for focal adhesions in MVcl-expressing fibroblasts (22). It is possible that the lack of statistical

significance in our experimental results arise from two factors. The first is inconsistent transfection efficiencies between independent experiments. The second is the fact that H9C2 cells are really large and it does not allow the sampling of too many individual cells for analysis. When we tried to increase the cell numbers suitable for FA analysis, the cells clustered on top of each other imposing problems with focal adhesion image analysis. Therefore, it would be nice in the future to repeat these experiments with stably generated cell lines in order to obtain statistically significant results.

Cardiac myocytes endure hypertrophic growing in response to an increase in work-load to maintain/increase cardiac activity. This can degenerate into heart failure and decompensation, a reaction that is followed by increased fibrosis. Hypertrophy of cardiac myocytes is correlated with morphological changes and gene/protein expression changes (35). A number of factors, such as vasoactive peptides, growth factors, cytokines, and hormones, cause cardiac hypertrophy. Catechol amines, including phenylephrine (PE) and isoproterenol (ISO), play a key role in cellular growth and cause cardiac hypertrophy (36,37). Isoproterenol is a ß-adrenoceptor agonist in the general class of synthetic which is one of the causative factors for permanent damage to the myocardial membrane. It creates free radicals and induces lipid peroxidation (38). On the other hand, phenylephrine, an α-adrenergic agonists activate particular receptors and actively stimulate intracellular signaling pathways, and also promote hypertrophy (35).

Given that the vinculin is listed as one of the familial hypertrophic cardiomyopathy genes, we investigated the effect of vinculin and metavinculin expression on the response of H9C2 cells to hypertrophy focusing on the changes in cellular morphology and focal adhesion areas. Hypertrophy was induced with isoproterenol and phenylephrine and were both successful as seen by an increase in cell size (according to FSC parameter) measured by flow cytometry (Figure 20). As can be seen from the FSC values in Figure 20, both drugs induced hypertrophy in 24 and 48 hours. Best results were obtained on the 2nd day of hypertrophy with the lowest doses of 10μM iso and 100 μM pe to avoid cytotoxic effects. Since both reagents were effective and commonly used for hypertrophy induction, we decided to perform our

functional experiments with isopretenol only. Furthermore, fluorescent microscope analysis of F-actin stained by Rhodamine or Alexa Fluor 488 Phalloidin demonstrated the alterations in cytoskeletal organization due to hypertrophic response in the presence of iso and pe agents (Figure 19).

The effect of metavinculin expression in response to hypertrophy was analyzed by comparing cell and focal adhesion areas to vinculin expressing cells. As seen earlier, MVcl-GFP expressing cells had larger cell size compared to Vcl-GFP expressing cells. However, the cells expressing MVcl-GFP and Vcl-GFP under hyprethrophic conditions did not show any difference in cell morphology or focal adhesion area. As seen in our earlier experiments, inconsistent transfection efficiency may reduce reproducibly. In addition, it was difficult to calculate cell areas in hypertrophic cells due to their inherent abnormal ultrastucture.

Vinculin is an adaptor protein that undergoes a to an open, active conformation when it is recruited to FAs leading to conformational rearrangements in its head and tail domains (39–41). This activation mechanism is essential for talin and alpha-actinin to have complete access to the head and paxillin to have direct contact with the tail (42). Therefore, we investigated the effect of vinculin and metavinculin expression on the levels of known focal adhesion proteins, FAK, Talin-1 and α-Actinin western blot analysis was performed under normal and hypertrophic conditions. Based on this analysis, we did not observe statistically significant differences between control and vinculin expressing cells in terms of FAK, Talin-1 and α-Actinin protein levels (Fig. 25). Fortes et al. found some results suggesting that β-actin is affected by hypertrophy. In this context, GAPDH was used as a housekeeping gene in hypertrophy western blot experiments (43). In summary, the target protein levels were generally lower under hypertrophy condiditons. Protein yield obtained from transfected cells was generally very low reducing the reproducibility in western blot analysis.

6 CONCLUSION

To summarize, the effect of metavinculin on the cell morphology and focal adhesions were presented for a cardiomyocyte cell line. It was concluded that metavinculin expression led to an increase in cell size compared to vinculin expressing cells. Although the total area of focal adhesions per cell were increased for metavinculin expressing cells, transient tranfection limited the reproducibility in our experiments. It was found that in case of hypertrophy, cells overexpressing vinculin and metavinculin had similar cell size and focal adhesions. In the future, the established methodology can be used in experiments designed with an alternative cell line or stably transfected H9C2 cells.

7 REFERENCES

1. World Health Organization (WHO). Cardiovascular diseases (CVDs) 2021 [internet]. Geneva: WHO; 2006.
2. Centers for Disease Control and Prevention. Heart Disease Statistics and Maps 2021 [internet]. Atlanta: CDC; 1946.
3. Maron BJ, Towbin JA, Thiene G, Antzelevitch C, Corrado D, Arnett D, et al. Contemporary definitions and classification of the cardiomyopathies: An American Heart Association Scientific Statement from the Council on Clinical Cardiology, Heart Failure and Transplantation Committee; Quality of Care and Outcomes Research and Functio. Circulation. 2006;113(14):1807–16.
4. Hershberger RE, Cowan J, Morales A, Siegfried JD. Progress with genetic cardiomyopathies; Screening, counseling, and testing in dilated, hypertrophic, and arrhythmogenic right ventricular dysplasia/cardiomyopathy. Circ Hear Fail. 2009;2(3):253–61.
5. Jefferies JL, Towbin JA. Dilated cardiomyopathy. Lancet. 2010;375(9716):752–62.
6. Peng X, Nelson ES, Maiers JL, DeMali KA. New insights into vinculin function and regulation. Int Rev Cell Mol Biol [Internet]. 2011;287:191–231.
7. Maziveyi M, Alahari SK, Maziveyi M, Alahari SK. Cell matrix adhesions in cancer: The proteins that form the glue. Oncotarget [Internet]. 2015;8(29):48471–87.
8. Hazan RB, Kang L, Roe S, Borgen PI, Rimm DL. Vinculin is associated with the E-cadherin adhesion complex. J Biol Chem [Internet]. 1997 Dec 19;272(51):32448–53.
9. Twiss F, Le Duc Q, Van Der Horst S, Tabdili H, Van Der Krogt G, Wang N, et al. Vinculin-dependent Cadherin mechanosensing regulates efficient epithelial barrier formation. Biol Open. 2012;1(11):1128–40.
10. Zemljic-Harpf AE, Ponrartana S, Avalos RT, Jordan MC, Roos KP, Dalton ND, et al. Heterozygous Inactivation of the Vinculin Gene Predisposes to Stress-Induced Cardiomyopathy. Am J Pathol. 2004;165(3):1033–44.
11. Belkin AM, Ornatsky OI, Kabakov AE, Glukhova MA, Koteliansky VE. Diversity of vinculin/meta-vinculin in human tissues and cultivated cells. Expression of muscle specific variants of vinculin in human aorta smooth muscle cells. J Biol Chem. 1988;263(14):6631–5.
12. Vasile VC, Ommen SR, Edwards WD, Ackerman MJ. A missense mutation in a ubiquitously expressed protein, vinculin, confers susceptibility to hypertrophic cardiomyopathy. Biochem Biophys Res Commun. 2006;345(3):998–1003.
13. Vasile VC, Will ML, Ommen SR, Edwards WD, Olson TM, Ackerman MJ. Identification of a metavinculin missense mutation, R975W, associated with both hypertrophic and dilated cardiomyopathy. Mol Genet Metab. 2006;87(2):169–74.
14. Rangarajan ES, Izard T. The cryogenic electron microscopy structure of the cell adhesion regulator metavinculin reveals an isoform-specific kinked helix in its cytoskeleton binding domain. Int J Mol Sci. 2021 Jan 2;22(2):1–18.

15. Oztug Durer ZA, McGillivary RM, Kang H, Elam WA, Vizcarra CL, Hanein D, et al. Metavinculin Tunes the Flexibility and the Architecture of Vinculin-Induced Bundles of Actin Filaments. J Mol Biol. 2015;427(17):2782–98.
16. Dadson K, Hauck L, Billia F. Molecular mechanisms in cardiomyopathy. Clin Sci. 2017;131(13):1375–92.
17. Braunwald E. Cardiomyopathies: An overview. Circ Res. 2017;121(7):711–21.
18. Brieler JAY, Breeden MA, Tucker J, Louis S. Cardiomyopathy: An Overview. 2017;
19. Paranal RM, Teekakirikul P, Ho CY, Fatkin D, Seidman CE. Genetic cardiomyopathies. Seventh Ed. Emery and Rimoin's Principles and Practice of Medical Genetics and Genomics: Cardiovascular, Respiratory, and Gastrointestinal Disorders. Elsevier; 2019. 77–114 p.
20. Maron BJ, Maron MS, Semsarian C. Genetics of hypertrophic cardiomyopathy after 20 years: Clinical perspectives. J Am Coll Cardiol. 2012;60(8):705–15.
21. Olson TM, Illenberger S, Kishimoto NY, Huttelmaier S, Keating MT, Jockusch BM. Metavinculin mutations alter actin interaction in dilated cardiomyopathy. Circulation. 2002;105(4):431–7.
22. Lee HT, Sharek L, O'Brien ET, Urbina FL, Gupton SL, Superfine R, et al. Vinculin and metavinculin exhibit distinct effects on focal adhesion properties, cell migration, and mechanotransduction. PLoS One [Internet]. 2019;14(9):e0221962.
23. Zemljic-Harpf AE, Miller JC, Henderson SA, Wright AT, Manso AM, Elsherif L, et al. Cardiac-Myocyte-Specific Excision of the Vinculin Gene Disrupts Cellular Junctions, Causing Sudden Death or Dilated Cardiomyopathy. Mol Cell Biol. 2007;27(21):7522–37.
24. Marg S, Winkler U, Sestu M, Himmel M, Schönherr M, Bär J, et al. The vinculin-Δin20/21 mouse: Characteristics of a constitutive, actin-binding deficient splice variant of vinculin. PLoS One. 2010;5(7).
25. Sarker M, Lee HT, Mei L, Krokhotin A, de los Reyes SE, Yen L, et al. Cardiomyopathy Mutations in Metavinculin Disrupt Regulation of Vinculin-Induced F-Actin Assemblies. J Mol Biol. 2019 Apr 5;431(8):1604–18.
26. Belkin AM, Ornatsky OI, Glukhova MA, Koteliansky VE. Immunolocalization of meta-vinculin in human smooth and cardiac muscles. J Cell Biol [Internet]. 1988;107(2):545–53.
27. Saga S, Hamaguchi M, Hoshino M, Kojima K. Expression of meta-vinculin associated with differentiation of chicken embryonal muscle cells. Exp Cell Res [Internet]. 1985;156(1):45–56.
28. Zemljic-Harpf AE, Godoy JC, Platoshyn O, Asfaw EK, Busija AR, Domenighetti AA, et al. Vinculin directly binds zonula occludens-1 and is essential for stabilizing connexin-43-containing gap junctions in cardiac myocytes. J Cell Sci. 2014;127(5):1104–16.
29. Horzum U, Ozdil B, Pesen-Okvur D. Step-by-step quantitative analysis of focal adhesions. MethodsX. 2014 Jan 1;1(1):56–9.
30. Watkins SJ, Borthwick GM, Arthur HM. The H9C2 cell line and primary neonatal cardiomyocyte cells show similar hypertrophic responses in vitro. Vitr Cell Dev Biol - Anim. 2011;47(2):125–31.
31. Zemljic-Harpf A, Manso AM, Ross RS. Vinculin and talin: focus on the myocardium. J Investig Med [Internet]. 2009;57(8):849–55.

32. Rothenberg KE, Scott DW, Christoforou N, Hoffman BD. Vinculin Force-Sensitive Dynamics at Focal Adhesions Enable Effective Directed Cell Migration. Biophys J [Internet]. 2018;114(7):1680–94.
33. American Type Culture Collection (ATCC). H9c2(2-1) 2022 [internet]. Manassas: ATCC.
34. Longo PA, Kavran JM, Kim MS, Leahy DJ. Transient mammalian cell transfection with polyethylenimine (PEI) [Internet]. 1st ed. Vol. 529, Methods in Enzymology. Elsevier Inc.; 2013. 227–240 p.
35. Kemp TJ, Aggeli IK, Sugden PH, Clerk A. Phenylephrine and endothelin-1 upregulate connective tissue growth factor in neonatal rat cardiac myocytes. J Mol Cell Cardiol [Internet]. 2004;37(2):603–6.
36. Hahn NE, Musters RJP, Fritz JM, Pagano PJ, Vonk ABA, Paulus WJ, et al. Early NADPH oxidase-2 activation is crucial in phenylephrine-induced hypertrophy of H9c2 cells. Cell Signal [Internet]. 2014;26(9):1818–24.
37. Jeong K, Kwon H, Min C, Pak Y. Modulation of the caveolin-3 localization to caveolae and STAT3 to mitochondria by catecholamine-induced cardiac hypertrophy in H9c2 cardiomyoblasts. Exp Mol Med. 2009;41(4):226–35.
38. Han D, Wan C, Liu F, Xu X, Jiang L, Xu J. Jujuboside A Protects H9C2 Cells from Isoproterenol-Induced Injury via Activating PI3K/Akt/mTOR Signaling Pathway. Evidence-based Complement Altern Med. 2016;2016.
39. Eimer, W. Niermann, M.Eppe, M. A.Jockusch BM. Molecular Shape of Vinculin in Aqueous Solution. J Mol Biol. 1993;229(1):146–52.
40. Winkler J, Lünsdorf H, Jockusch BM. The ultrastructure of chicken gizzard vinculin as visualized by high-resolution electron microscopy. J Struct Biol. 1996;116(2):270–7.
41. Cohen DM, Chen H, Johnson RP, Choudhury B, Craig SW. Two distinct head-tail interfaces cooperate to suppress activation of vinculin by talin. J Biol Chem [Internet]. 2005;280(17):17109–17.
42. Humphries JD, Wang P, Streuli C, Geiger B, Humphries MJ, Ballestrem C. Vinculin controls focal adhesion formation by direct interactions with talin and actin. J Cell Biol. 2007;179(5):1043–57.
43. Fortes MAS, Marzuca-Nassr GN, Vitzel KF, Da Justa Pinheiro CH, Newsholme P, Curi R. Housekeeping proteins: How useful are they in skeletal muscle diabetes studies and muscle hypertrophy models? Anal Biochem. 2016;504:38–40.

8 CURRICULUM VITAE